

This preprint has been submitted for publication in the International Journal of Robotics Research (IJRR).

First submission: 12 October 2024

<https://journals.sagepub.com/home/ijr>

The Indirect Method for Generating Libraries of Optimal Periodic Trajectories and Its Application to Economical Bipedal Walking

Journal Title
XX(X):2–16
©The Author(s) 2024
Reprints and permission:
sagepub.co.uk/journalsPermissions.nav
DOI: 10.1177/ToBeAssigned
www.sagepub.com/


Maximilian Raff ¹, Kathrin Flaßkamp ², C. David Remy ¹

Abstract

Trajectory optimization is an essential tool for generating efficient and dynamically consistent gaits in legged locomotion. This paper explores the indirect method of trajectory optimization, emphasizing its application in creating optimal periodic gaits for legged systems and contrasting it with the more commonly used direct method. While the direct method provides considerable flexibility in its implementation, it is limited by its input space parameterization. In contrast, the indirect method improves accuracy by defining control inputs as functions of the system's states and costates. We tackle the convergence challenges associated with indirect shooting methods, particularly through the systematic development of gait libraries by utilizing numerical continuation methods. Our contributions include: (1) the formalization of a general periodic trajectory optimization problem that extends existing first-order necessary conditions for a broader range of cost functions and operating conditions; (2) a methodology for efficiently generating libraries of optimal trajectories (gaits) utilizing a single shooting approach combined with numerical continuation methods, including a novel approach for reconstructing Lagrange multipliers and costates from passive gaits; and (3) a comparative analysis of the indirect and direct shooting methods using a compass-gait walker as a case study, demonstrating the former's superior accuracy in generating optimal gaits. The findings underscore the potential of the indirect method for generating families of optimal gaits, thereby advancing the field of trajectory optimization in legged robotics.

Keywords

Variational Approach, Trajectory Optimization, Single Shooting, Legged Robotics, Numerical Continuation, Gait Library

1 Introduction

Optimal control is widely used for path and motion planning in robotics. This holds in particular in the field of legged robotic systems, where the creation of efficient, stable, and dynamically consistent gaits is a crucial ability. Trajectory optimization has thus become an essential tool for design and control in applications that reach from humanoid robots to exoskeletons and prosthetics (Wensing et al. 2024).

Methods for optimal control are classified into *direct* and *indirect*. The *direct method* is the most commonly used for trajectory optimization. In this method, control inputs are parameterized and optimized directly over a predefined input space (Diehl et al. 2006; Kelly 2017; Wensing et al. 2024). While this discretization increases the dimensionality of the optimization problem, the approach is straightforward and offers considerable flexibility in terms of implementation. As a drawback, the accuracy of the resulting optimal trajectory depends on the chosen parameterization of the input space, potentially missing better solutions that exist outside this discretization. This leads to a trade-off between accuracy and problem size, while the true global optimum may remain unattainable due to the constraints imposed by the parameterization (Houska and Chachuat 2013; Lin et al. 2014). The *indirect method* offers a different approach by implicitly defining the control inputs as functions of the system's states and additional costates. It often provides more accurate solutions, especially when

using shooting methods with variable step-size integrators. While the introduction of costates helps formalize the first-order necessary conditions, it does not significantly increase the dimensionality of the optimization problem. The challenge of the indirect method, however, lies in the numerical convergence, primarily due to the conservative dynamics of the Hamiltonian system (Gros and Diehl 2022). Specifically, stable modes in the system's dynamics are often counterbalanced by unstable modes in the costate dynamics, leading to convergence difficulties (von Stryk and Bulirsch 1992; Betts 2010; Gros and Diehl 2022; Wensing et al. 2024).

Although the indirect method in periodic trajectory optimization has been used in fields such as aerospace (Gilbert and Lyons 1981; Speyer 1996) and hybrid systems in chemical processes (Horn and Lin 1967), it has not achieved the same popularity as the direct method. An example from legged locomotion is the work by Channon et al. (1996) on bipedal walking. However, this work utilized collocation techniques, a

¹Institute for Nonlinear Mechanics, University of Stuttgart, Germany.

²Systems Modeling and Simulation, Saarland University, Germany

Corresponding author:

Maximilian Raff, Institute for Nonlinear Mechanics, University of Stuttgart, Pfaffenwaldring 9, 70569 Stuttgart, Germany.
Email: raff@inm.uni-stuttgart.de

common approach for extending the convergence region of the indirect method (von Stryk and Bulirsch 1992). Unfortunately, combining the indirect method with collocation or fixed step-size shooting diminishes its core advantage, making it nearly equivalent to the direct method in terms of accuracy (Ross 2020), and thus losing its potential for achieving higher precision in solving optimal control problems. In addition, Channon et al. (1996) does not incorporate cost functions that normalize over the period of the gait cycle. These cost functions, commonly used in periodic trajectory optimization (Colonius 1988; Speyer and Evans 1984; Horn and Lin 1967), are crucial in assessing measures like cost of transport, which are key performance metrics in legged locomotion.

A key insight of this work is that in legged robotics, we are often interested not only in a single solution but in generating libraries of optimal gaits that adapt to varying conditions, such as changes in terrain or the robot's speed. When considering such parameterized optimization problems, numerical continuation methods can quickly generate many gaits. These continuation methods offer robust local convergence properties and can help overcome the challenges typically associated with the indirect method and –by pairing it with a single shooting approach– hold promise for generating families of optimal gaits with higher accuracy than with direct methods. In prior work, we showed that such parameterized optimization problems may exhibit *passive gaits*, which are especially relevant as they trivially solve certain economic optimization problems by minimizing energy consumption without requiring active control inputs (Raff et al. 2022; Rosa et al. 2023). Such passive gaits could be leveraged as seeds for a gait library, if we can reconstruct states, costates, and Lagrange multipliers as they are needed in the indirect method.

This paper explores these ideas and makes several contributions to trajectory optimization for systems with hybrid dynamics, particularly in legged locomotion:

- **Formalization of a General Trajectory Optimization Problem:** We extend the first-order necessary conditions from the existing literature to a broader class of cost functions and operating conditions, addressing both legged systems and other periodically operating robots with hybrid dynamics.
- **Generation of Gait Libraries with Lagrange Multiplier and Costate Reconstruction:** By reformulating the first-order necessary conditions as parameter-dependent root-finding problems and applying a single shooting method, we develop a robust framework to generate and analyze families of optimal gaits using numerical continuation techniques.
- **Performance Evaluation of the Indirect Method:** Using a compass-gait walker as case study, we compare the indirect shooting method with the direct shooting method. The results highlight the indirect method's superior accuracy and its effectiveness in managing input space parameterization, showcasing its advantages for generating optimal gaits in systems with hybrid dynamics.

The remainder of this paper is organized as follows. In Section 2, we formalize a generic trajectory optimization

problem applicable to legged systems and other periodically operating robots. This section includes a detailed derivation of the first-order necessary conditions for optimality using the Calculus of Variations and the Lagrange multiplier method. We then extend the optimization framework to incorporate a set of parameters that characterize families of optimal gaits, concluding with a discussion on how to reconstruct Lagrange multipliers from passive periodic solutions within these gait families. In Section 3, we discuss the implementation of single-shooting methods and numerical continuation techniques for tracing solution curves within the parameterized optimization problem. Section 4 presents the compass-gait walker as a case study, applying the indirect shooting method to bipedal walking. This section demonstrates how to generate families of optimal gaits that originate from passive gaits, and compares the indirect method to direct shooting approaches. Section 5 concludes the paper and is followed by an appendix that provides detailed derivations of the first-order optimality conditions (Appendix A.1), the dynamics of the compass-gait walker (Appendix A.2), and additional details on the implementation of the direct shooting method (Appendix A.3).

2 Theory

In this section, we formalize a generic trajectory optimization problem applicable to legged systems as well as other periodically operating robots and mechanisms that may involve non-smooth interactions with the environment. We present a detailed derivation of the first-order necessary conditions using the Calculus of Variations, incorporating the Lagrange multiplier method. The section concludes with a parameterization for a library of optimal trajectories and a discussion on reconstructing Lagrange multipliers from passive periodic solutions.

To avoid notational overhead, we omit the argument of a function when it is clear from the context, writing α instead of $\alpha(t)$. Otherwise, we use the shorthand notation $\alpha_t = \alpha(t)$.

2.1 Problem Formulation

The purpose of a periodic trajectory optimization problem is to find a period time $T \in \mathbb{R}$, a state trajectory $\mathbf{x}(\cdot)$, with $\mathbf{x}(t) \in \mathbb{R}^{n_x}$, and an input trajectory $\mathbf{u}(\cdot)$, with $\mathbf{u}(t) \in \mathbb{R}^{n_u}$, where $t \in [0, T]$, that (locally) minimize the trajectory optimization problem \mathcal{P} (see box below).

The problem \mathcal{P} is written in a general Mayer form (Liberzon 2011), which is characterized by a terminal cost function $c : \mathbb{R} \times \mathbb{R}^{n_x} \times \mathbb{R} \rightarrow \mathbb{R}$. In this framework, the auxiliary state $\mathbf{y}(\cdot)$, with $\mathbf{y}(t) \in \mathbb{R}$, accumulates the stage cost over time through the function $l : \mathbb{R}^{n_x} \times \mathbb{R}^{n_u} \rightarrow \mathbb{R}$. Consequently, $y(T)$ represents the total accumulated stage cost, which can then be incorporated into the Mayer-type cost function. Additionally, \mathcal{P} includes dynamic constraints representing a simple hybrid system (Ames 2006), which consists of both continuous and discrete dynamics in a single phase. The continuous evolution is governed by the ordinary differential equation (1b) with vector field $\mathbf{f} : \mathbb{R}^{n_x} \times \mathbb{R}^{n_u} \rightarrow \mathbb{R}^{n_x}$, while the discrete transitions are modeled by the reset map $\mathbf{g} : \mathbb{R}^{n_x} \rightarrow \mathbb{R}^{n_x}$ in equation (1c), which also defines

Periodic Trajectory Optimization Problem \mathcal{P}	
minimize	$c(T, \mathbf{x}(T), y(T))$
$T, \mathbf{x}(\cdot), \mathbf{u}(\cdot)$	(1a)
subject to	$\dot{\mathbf{x}}(t) = \mathbf{f}(\mathbf{x}(t), \mathbf{u}(t)), \quad t \in [0, T],$
	(1b)
	$\mathbf{x}(0) = \mathbf{g}(\mathbf{x}(T)),$
	(1c)
	$\dot{y}(t) = l(\mathbf{x}(t), \mathbf{u}(t)), \quad t \in [0, T],$
	(1d)
	$y(0) = 0,$
	(1e)
	$\underbrace{\begin{bmatrix} e(T, \mathbf{x}(T), \mathbf{x}(0)) \\ \omega(T, \mathbf{x}(T), \mathbf{x}(0)) \end{bmatrix}}_{= \mathbf{h}(T, \mathbf{x}(T), \mathbf{x}(0))} = \mathbf{0}, \quad (1f)$

the system's periodicity. The guard condition associated with these discrete transitions is provided by the event constraint $e : \mathbb{R} \times \mathbb{R}^{n_x} \times \mathbb{R}^{n_x} \rightarrow \mathbb{R}$. This event is typically tied to the final state $\mathbf{x}(T)$ and final time T , but due to the periodic nature of the system, it may also be related to the initial state $\mathbf{x}(0)$ as in Channon et al. (1996). The equality constraint $\mathbf{h} : \mathbb{R} \times \mathbb{R}^{n_x} \times \mathbb{R}^{n_x} \rightarrow \mathbb{R}^{1+n_\omega}$ in equation (1f) encompasses both the event constraint e and an operating point constraint $\omega : \mathbb{R} \times \mathbb{R}^{n_x} \times \mathbb{R}^{n_x} \rightarrow \mathbb{R}^{n_\omega}$, imposing n_ω operating conditions. The operating point typically defines desired amplitudes and frequencies, or metrics such as average system energy and velocities. Introducing an operating point is essential for generating motions with user-defined characteristics, especially when optimizing for energetic efficiency. It actively avoids trivial optimal solutions that correspond to either no motion (equilibria) or zero time duration ($T = 0$).

Before we derive the equations for the first-order optimality of \mathcal{P} with the indirect method, we state the following assumptions.

Assumption Existence of Local Extrema. *The optimization problem \mathcal{P} admits at least one strict local minimizer ($T^* > 0, \mathbf{x}^*(\cdot), \mathbf{u}^*(\cdot)$).*

Assumption Differentiability. *The control input is continuous, i.e., $\mathbf{u} \in C^0$, and unconstrained. The functions $c(\cdot, \cdot, \cdot)$, $\mathbf{f}(\cdot, \cdot)$, $l(\cdot, \cdot)$, $\mathbf{g}(\cdot)$ and $\mathbf{h}(\cdot, \cdot, \cdot)$ are of class C^∞ with respect to all arguments.*

While the continuity assumption on the input \mathbf{u} can be relaxed (Speyer and Evans 1984; Liberzon 2011) using Pontryagin's maximum principle (Pontryagin 1987), this is beyond the scope of this paper. Additionally, we restrict ourselves to equality constraints in \mathcal{P} . A potential extension to include inequality constraints on the states \mathbf{x} and inputs \mathbf{u} is discussed in the concluding Section 5.

2.2 Derivation of the First-Order Necessary Condition

To formalize the first-order necessary conditions of problem \mathcal{P} , we utilize Lagrange's multiplier method for the so-called non-integral (1b), (1d) and integral constraint equations (1c), (1e), (1f) (Liberzon 2011). The non-integral equality constraints (1b) and (1d) must hold

point-wise in time for all $t \in [0, T]$. They introduce continuous time Lagrange multipliers, referred to as the costates $\mathbf{p} \in \mathbb{R}^{n_x}$ and $q \in \mathbb{R}$ of \mathbf{x} and y , respectively. The integral equality constraints (1f) also introduce Lagrange multipliers $\lambda^T = [\lambda_e \ \lambda_\omega^T] \in \mathbb{R}^{1+n_\omega}$. However, these multipliers are discrete in time, as they act at constraints that depend only on the states at the boundary of the trajectory. Similarly, for the integral equality constraints (1c) and (1e), we introduce Lagrange multipliers $z\lambda^T = [z\lambda^T \ y\lambda] \in \mathbb{R}^{n_x}$ and $y\lambda \in \mathbb{R}$.

For notational convenience, we group the continuous and discrete time variables as

$$\mathbf{z}(\cdot)^T = [\mathbf{x}(\cdot)^T \ y(\cdot)], \quad (2a)$$

$$\boldsymbol{\rho}(\cdot)^T = [\mathbf{p}(\cdot)^T \ q(\cdot)], \quad (2b)$$

$$\mathbf{w}(\cdot)^T = [\mathbf{z}(\cdot)^T \ \boldsymbol{\rho}(\cdot)^T \ \mathbf{u}(\cdot)^T], \quad (2c)$$

$$\mathbf{v}^T = [T \ \lambda^T], \quad (2d)$$

and define the Hamiltonian as

$$\mathcal{H}(\underbrace{\mathbf{x}, y, \mathbf{p}, q, \mathbf{u}}_{= \mathbf{w}}) = \mathbf{p}^T \mathbf{f}(\mathbf{x}, \mathbf{u}) + q \cdot l(\mathbf{x}, \mathbf{u}). \quad (3)$$

With the introduction of these Lagrange multipliers, the Lagrangian is defined as

$$L(z\lambda, \mathbf{v}, \mathbf{w}(\cdot)) = L_1(\mathbf{v}, \mathbf{w}) + L_2(z\lambda, \mathbf{w}) + L_3(\mathbf{v}, \mathbf{w}), \quad (4a)$$

where

$$L_1 = c(T, \mathbf{z}(T)) + \lambda^T \mathbf{h}(T, \mathbf{x}(T), \mathbf{x}(0)), \quad (4b)$$

$$L_2 = z\lambda^T (\mathbf{g}(\mathbf{x}(T)) - \mathbf{x}(0)) + y\lambda y(0), \quad (4c)$$

$$L_3 = \int_0^T \mathcal{H}(\mathbf{w}) - \boldsymbol{\rho}^T \dot{\mathbf{z}} dt, \quad (4d)$$

With the Lagrangian, the stationarity condition within the constrained optimization problem \mathcal{P} can be equivalently written as an unconstrained problem (Kalman 2009):

$$\text{stationary } \underset{z\lambda, \mathbf{v}, \mathbf{w}(\cdot)}{L}(z\lambda, \mathbf{v}, \mathbf{w}(\cdot)). \quad (5)$$

To derive the stationarity condition of the new problem (5), we perturb its solution $(z\lambda^*, \mathbf{v}^*, \mathbf{w}^*)$ with $\delta z\lambda^T = [\delta z\lambda^T \ \delta y\lambda]$, $\delta \mathbf{v}^T = [\delta T \ \delta \lambda^T]$ and $\delta \mathbf{w}(\cdot)^T = [\delta \mathbf{z}(\cdot)^T \ \delta \mathbf{u}(\cdot)^T \ \delta \boldsymbol{\rho}(\cdot)^T]$ such that

$$\begin{aligned} z\tilde{\lambda} &= z\lambda^* + \varepsilon \delta z\lambda, \\ \tilde{\mathbf{v}} &= \mathbf{v}^* + \varepsilon \delta \mathbf{v}, \\ \tilde{\mathbf{w}}(\cdot) &= \mathbf{w}^*(\cdot) + \varepsilon \delta \mathbf{w}(\cdot), \end{aligned} \quad (6)$$

where ε is infinitesimally small. Note that $\mathbf{w}(t)$ is a function of time and is thus, coupled to the variation of the period time T in \mathbf{v} at the end of the trajectory:

$$\begin{aligned} \tilde{\mathbf{w}}(\tilde{T}) &= \mathbf{w}^*(\tilde{T}) + \varepsilon \delta \mathbf{w}(\tilde{T}) \\ &= \mathbf{w}^*(T^* + \varepsilon \delta T) + \varepsilon \delta \mathbf{w}(T^* + \varepsilon \delta T). \end{aligned} \quad (7)$$

At a locally optimal point of problem \mathcal{P} , the first variation $\delta L|_*$ of the Lagrangian (4) must vanish. With

$\tilde{L}(\varepsilon) := L(z\tilde{\lambda}, \tilde{v}, \tilde{w}(\cdot))$, the stationary condition takes the form

$$\delta L|_* := \frac{\partial \tilde{L}(\varepsilon)}{\partial \varepsilon} \Big|_{\varepsilon=0} = 0. \quad (8)$$

Remark 2.1. To formulate the unconstrained problem (5) using Lagrange multipliers, certain regularity conditions on the equality constraints are required. We have not introduced the notion of regularity here, as it involves technical details specific to the infinite-dimensional vector spaces under consideration. For a thorough discussion on the required regularity conditions, please refer to Chapter 9.2 of Luenberger (1997).

Executing the first-order variation, as detailed in Appendix A.1, and omitting the superscript $*$, yields the following expression:

$$\begin{aligned} 0 &= \delta L \\ &= \int_0^T \left(\left[\frac{\partial \mathcal{H}}{\partial \mathbf{z}} + \dot{\mathbf{p}}^T \right] \delta \mathbf{x} + \left[\frac{\partial \mathcal{H}}{\partial \mathbf{p}} - \dot{\mathbf{z}}^T \right] \delta y \right) dt \\ &\quad + \int_0^T \left(\left[\frac{\partial \mathcal{H}}{\partial \mathbf{u}} \right] \delta \mathbf{u} \right) dt \\ &\quad + \left[\delta \mathbf{z}_0^T \quad \delta \mathbf{z}_T^T \quad \delta T \quad \delta \mathbf{\lambda}^T \quad \delta_z \mathbf{\lambda}^T \right] \cdot \delta \tilde{\mathbf{r}}, \end{aligned} \quad (9a)$$

where

$$\delta \tilde{\mathbf{r}}^T = \begin{bmatrix} z_0 \tilde{\mathbf{r}}^T & z_T \tilde{\mathbf{r}}^T & T \tilde{\mathbf{r}} & \mathbf{h}^T & z \mathbf{h}^T \end{bmatrix}, \quad (9b)$$

$$z_0 \tilde{\mathbf{r}}^T = \begin{bmatrix} x_0 \tilde{\mathbf{r}}^T & y_0 \tilde{\mathbf{r}} \end{bmatrix} \quad (9c)$$

$$z_T \tilde{\mathbf{r}}^T = \begin{bmatrix} x_T \tilde{\mathbf{r}}^T & y_T \tilde{\mathbf{r}} \end{bmatrix} \quad (9d)$$

$$z \mathbf{h}^T = \begin{bmatrix} (\mathbf{g}(\mathbf{x}_T) - \mathbf{x}_0)^T & y_0 \end{bmatrix}, \quad (9e)$$

with

$$x_0 \tilde{\mathbf{r}} = \frac{\partial \mathbf{h}^T}{\partial \mathbf{x}_0} \mathbf{\lambda} + \mathbf{p}_0 - x \mathbf{\lambda}, \quad (9f)$$

$$y_0 \tilde{\mathbf{r}} = q_0 + y \lambda, \quad (9g)$$

$$x_T \tilde{\mathbf{r}} = \frac{\partial \mathbf{g}^T}{\partial \mathbf{x}_T} x \mathbf{\lambda} - \mathbf{p}_T + \frac{\partial c^T}{\partial \mathbf{x}_T} + \frac{\partial \mathbf{h}^T}{\partial \mathbf{x}_T} \mathbf{\lambda}, \quad (9h)$$

$$y_T \tilde{\mathbf{r}} = \frac{\partial c}{\partial y_T} - q_T, \quad (9i)$$

$$T \tilde{\mathbf{r}} = \mathcal{H}(\mathbf{w}_T) + \frac{\partial c}{\partial T} + \mathbf{\lambda}^T \frac{\partial \mathbf{h}}{\partial T} \quad (9j)$$

$$+ x_T \tilde{\mathbf{r}}^T \cdot \dot{\mathbf{x}}_T + y_T \tilde{\mathbf{r}} \cdot \dot{y}_T. \quad (9k)$$

Since the problem (5) is unconstrained, the first-order variation (9a) must hold for arbitrary perturbations $\delta_z \mathbf{\lambda}$, $\delta \mathbf{v}$ and $\delta \mathbf{w}(\cdot)$. Thus, applying the fundamental lemma of the calculus of variations yields

$$\dot{\mathbf{p}}(t) = - \frac{\partial \mathcal{H}}{\partial \mathbf{z}} \Big|_{\mathbf{w}(t)}^T, \quad \dot{\mathbf{z}}(t) = \frac{\partial \mathcal{H}}{\partial \mathbf{p}} \Big|_{\mathbf{w}(t)}^T, \quad \mathbf{0} = \frac{\partial \mathcal{H}}{\partial \mathbf{u}} \Big|_{\mathbf{w}(t)}^T, \quad (10)$$

for all $t \in [0, T]$ and requires the residual equations (9b) to vanish:

$$\begin{bmatrix} x_0 \tilde{\mathbf{r}}^T & y_0 \tilde{\mathbf{r}} & x_T \tilde{\mathbf{r}}^T & y_T \tilde{\mathbf{r}} & T \tilde{\mathbf{r}} & \mathbf{h}^T & z \mathbf{h}^T \end{bmatrix} = \mathbf{0}. \quad (11)$$

While the differential equations (10) constitute the first part of the necessary conditions, equation (11) contains so-called transversality ($_i \tilde{\mathbf{r}}$) and boundary ($\mathbf{h}, z \mathbf{h}$) conditions. Notably, from equations (10) follows: $\dot{q} = -\partial \mathcal{H} / \partial y = 0$. This results in a constant Lagrange multiplier q which is derived from the transversality condition (9i) as $q(t) \equiv q_0 = q_T = \partial c / \partial y_T$. Likewise, the transversality conditions (9f) and (9g) can be rewritten as

$$_x \mathbf{\lambda} = \frac{\partial \mathbf{h}^T}{\partial \mathbf{x}_0} \mathbf{\lambda} + \mathbf{p}_0, \quad _y \lambda = -q. \quad (12)$$

Hence, $_x \mathbf{\lambda}$ can be eliminated from the transversality condition (9h). Finally, under the fulfillment of the residuals $_x \tilde{\mathbf{r}} = \mathbf{0}$ and $_y \tilde{\mathbf{r}} = 0$, the last transversality condition (9j) simplifies as its additive terms (9k) vanish. With these simplifications, equations (10) and (11) yield the first-order necessary conditions in the compact form presented in the box below.

First-Order Necessary Condition of Optimality

Utilizing calculus of variations, the first-order necessary condition of optimality for problem \mathcal{P} takes the form of a differential-algebraic system of equations (DAE):

$$\dot{\mathbf{x}} = \frac{\partial \mathcal{H}^T}{\partial \mathbf{p}} = \mathbf{f}(\mathbf{x}, \mathbf{u}), \quad (13a)$$

$$\dot{y} = \frac{\partial \mathcal{H}}{\partial q} = l(\mathbf{x}, \mathbf{u}), \quad (13b)$$

$$\dot{\mathbf{p}} = -\frac{\partial \mathcal{H}^T}{\partial \mathbf{x}} = -\frac{\partial \mathbf{f}^T}{\partial \mathbf{x}} \mathbf{p} - \frac{\partial l^T}{\partial \mathbf{x}} q, \quad (13c)$$

$$q \equiv \frac{\partial c}{\partial y_T}, \quad (13d)$$

$$\mathbf{0} = \frac{\partial \mathcal{H}^T}{\partial \mathbf{u}} = \frac{\partial \mathbf{f}^T}{\partial \mathbf{u}} \mathbf{p} + \frac{\partial l^T}{\partial \mathbf{u}} q, \quad (13e)$$

with associated boundary and transversality constraints:

$$\mathbf{g}(\mathbf{x}(T)) - \mathbf{x}(0) = \mathbf{0}, \quad (14a)$$

$$y(0) = 0, \quad (14b)$$

$$\mathbf{h}(T, \mathbf{x}(T), \mathbf{x}(0)) = \mathbf{0}, \quad (14c)$$

$$\mathcal{H}(\mathbf{w}(T)) + \frac{\partial c}{\partial T} + \mathbf{\lambda}^T \frac{\partial \mathbf{h}}{\partial T} = 0, \quad (14d)$$

$$\begin{aligned} \frac{\partial \mathbf{g}^T}{\partial \mathbf{x}_T} \cdot \left(\mathbf{p}(0) + \frac{\partial \mathbf{h}^T}{\partial \mathbf{x}_0} \mathbf{\lambda} \right) - \mathbf{p}(T) \\ + \frac{\partial c^T}{\partial \mathbf{x}_T} + \frac{\partial \mathbf{h}^T}{\partial \mathbf{x}_T} \mathbf{\lambda} = \mathbf{0}, \end{aligned} \quad (14e)$$

where the Hamiltonian is defined as

$$\mathcal{H}(\underbrace{\mathbf{x}, y, \mathbf{p}, q, \mathbf{u}}_{=\mathbf{w}}) = \mathbf{p}^T \mathbf{f}(\mathbf{x}, \mathbf{u}) + q \cdot l(\mathbf{x}, \mathbf{u}). \quad (15)$$

2.3 Parameterized Optimization Problem

In legged locomotion, there is a significant interest in generating libraries of gaits that adapt to varying

conditions which are represented by a parameter set $\sigma \in \mathbb{R}^{n_\sigma}$ (Reher and Ames 2021; Westervelt et al. 2018; Raff et al. 2022; Rosa et al. 2023). These parameters may represent environmental variations, such as changes in slope or terrain, as well as variations in the robot's operating conditions, such as forward speed or step length. Introducing these parameters in the optimization problem \mathcal{P} creates the parameterized optimization problem:

$$\mathcal{P}_\sigma \left\{ \begin{array}{ll} \text{minimize}_{T, \mathbf{x}(\cdot), \mathbf{u}(\cdot)} & c(T, \mathbf{x}(T), y(T); \sigma) \\ \text{subject to} & \dot{\mathbf{x}}(t) = \mathbf{f}(\mathbf{x}(t), \mathbf{u}(t); \sigma), \quad t \in [0, T], \\ & \mathbf{x}(0) = \mathbf{g}(\mathbf{x}(T); \sigma), \\ & \dot{y}(t) = l(\mathbf{x}(t), \mathbf{u}(t); \sigma), \quad t \in [0, T], \\ & y(0) = 0, \\ & \mathbf{h}(T, \mathbf{x}(T), \mathbf{x}(0); \sigma) = \mathbf{0}, \end{array} \right.$$

where we introduced some abuse of notation by not redefining the functions in equations (1). With the definition of \mathcal{P}_σ , the first-order optimality conditions (13), (14) are also parameterized by σ . Provided that a stationary point of \mathcal{P}_σ is regular (Remark 2.1) at a nominal parameter set $\bar{\sigma}$, there exists a locally defined manifold of optimal solutions parameterized by σ .

2.4 Reconstruction of Lagrange Multipliers

In contrast to the Lagrange multipliers $z\lambda$ defined in equations (12), the multipliers λ and $\rho(\cdot)$ can not be eliminated as easily. In general applications of the indirect method, determining the costates $\mathbf{p}(\cdot)$ is particularly challenging, as discussed, for example, by von Stryk and Bulirsch (1992) and in Chapter 4.4 of Betts (2010). In this paper, we exploit what we term *passive-optimal solutions*; that is, locally optimal solutions to the parameterized problem \mathcal{P}_σ with vanishing control inputs ($\mathbf{u} \equiv \mathbf{0}$). For such solutions, the costates can be reconstructed, and if they lie on the solution manifold described above, they can serve as initial conditions for a numerical continuation process to systematically explore the entire manifold.

Definition Passive-Optimal Solution. *A strict local minimizer $(T^*, \mathbf{x}^*(\cdot), \mathbf{u}^*(\cdot))$, with $\mathbf{u}^* \equiv \mathbf{0}$, at a fixed parameter vector $\bar{\sigma}$ for problem \mathcal{P}_σ , is referred to as a passive-optimal solution, or in the context of legged locomotion, a passive-optimal gait.*

Provided a passive-optimal solution, the multipliers λ and $\rho(\cdot)$ can be reconstructed via the necessary conditions (13) and (14). In particular, with the condition (13d), the first Lagrange multiplier can be readily reconstructed:

$$q = \frac{\partial c}{\partial y_T} \Big|_{(T^*, \mathbf{x}^*(T^*), y(T^*), \bar{\sigma})}, \quad (16)$$

where $y(T^*) = \int_0^{T^*} l(\mathbf{x}^*(t), \mathbf{0}, \bar{\sigma}) dt$. For the reconstruction of the costate trajectory $\mathbf{p}(\cdot)$, we reformulate the necessary conditions (13) to

$$\dot{\mathbf{w}} = \mathcal{F}(\mathbf{w}, \bar{\sigma}), \quad (17a)$$

$$\mathbf{0} = \mathcal{H}_u(\mathbf{w}, \bar{\sigma}), \quad (17b)$$

where

$$\mathcal{F} := \begin{bmatrix} \mathbf{f}(\mathbf{x}, \mathbf{u}, \bar{\sigma}) \\ l(\mathbf{x}, \mathbf{u}, \bar{\sigma}) \\ -\frac{\partial \mathbf{f}}{\partial \mathbf{x}} \Big|_{(\mathbf{x}, \mathbf{u}, \bar{\sigma})}^T \cdot \mathbf{p} - \frac{\partial l}{\partial \mathbf{x}} \Big|_{(\mathbf{x}, \mathbf{u}, \bar{\sigma})}^T \cdot q \\ 0 \\ \mathbf{0} \end{bmatrix}, \quad (18a)$$

$$\mathcal{H}_u := \frac{\partial \mathbf{f}}{\partial \mathbf{u}} \Big|_{(\mathbf{x}, \mathbf{u}, \bar{\sigma})}^T \cdot \mathbf{p} + \frac{\partial l}{\partial \mathbf{u}} \Big|_{(\mathbf{x}, \mathbf{u}, \bar{\sigma})}^T \cdot q. \quad (18b)$$

Note that the dynamics $\dot{\mathbf{u}} = \mathbf{0}$ in equations (18a) result from the passive inputs $\mathbf{u}^* \equiv \mathbf{0}$.

Since the costates $\mathbf{p}(\cdot)$ are uniquely associated to \mathbf{x}^* and \mathbf{u}^* by equations (17), they are locally observable within equations (17b) (Isidori 1995). Exploiting the fact that \mathbf{p} and q are affine in the vector field \mathcal{F} and in the function \mathcal{H}_u , we utilize the Lie derivative \mathcal{L} and define

$$\begin{bmatrix} \mathcal{H}_u \\ \mathcal{L}_F \mathcal{H}_u \\ \mathcal{L}_F \mathcal{L}_F \mathcal{H}_u \\ \vdots \end{bmatrix} \Big|_{(\mathbf{x}^*, \mathbf{p}, \mathbf{u}^*, \bar{\sigma})} = \tilde{\mathbf{A}}\mathbf{p} + \tilde{\mathbf{b}}q \stackrel{!}{=} \mathbf{0}, \quad (19a)$$

where

$$\tilde{\mathbf{A}} = \begin{bmatrix} \frac{\partial \mathbf{f}}{\partial \mathbf{u}}^T \\ \left(\sum_{i=1}^{n_x} f_i \frac{\partial}{\partial x_i} \frac{\partial \mathbf{f}}{\partial \mathbf{u}} \right)^T - \left(\frac{\partial \mathbf{f}}{\partial \mathbf{x}} \frac{\partial \mathbf{f}}{\partial \mathbf{u}} \right)^T \\ \vdots \end{bmatrix}, \quad (19b)$$

$$\tilde{\mathbf{b}} = \begin{bmatrix} \frac{\partial l}{\partial \mathbf{u}}^T \\ \left(\sum_{i=1}^{n_x} f_i \frac{\partial}{\partial x_i} \frac{\partial l}{\partial \mathbf{u}} \right)^T - \left(\frac{\partial l}{\partial \mathbf{x}} \frac{\partial \mathbf{f}}{\partial \mathbf{u}} \right)^T \\ \vdots \end{bmatrix}, \quad (19c)$$

are evaluated at the point $(\mathbf{x}^*, \mathbf{u}^*, \bar{\sigma})$. Due to the local observability of \mathbf{p} , the matrix $\tilde{\mathbf{A}}$ has full (column) rank for all $(\mathbf{x}^*(t), \mathbf{u}^*(t) = \mathbf{0})$ and $t \in [0, T^*]$. Thus, for each time instant, we can construct a square matrix $\mathbf{A}(t) \in \mathbb{R}^{n_x \times n_x}$ from n_x rows of $\tilde{\mathbf{A}}$ such that $\det(\mathbf{A}(t)) \neq 0$. Furthermore, selecting the same n_x rows from $\tilde{\mathbf{b}}$ constitutes the vector $\mathbf{b}(t) \in \mathbb{R}^{n_x}$. Finally, the costate can be reconstructed by

$$\mathbf{p}(t) = \mathbf{A}(t)^{-1} \mathbf{b}(t) q, \quad (20)$$

for any time $t \in [0, T^*]$. With the computed costates $\mathbf{p}(0)$ and $\mathbf{p}(T^*)$ at the boundary, the remaining Lagrange multipliers λ are reconstructed from equations (14e):

$$\begin{aligned} \lambda &= \mathbf{H}^+ \cdot \left(\mathbf{p}(T^*) - \frac{\partial \mathbf{g}}{\partial \mathbf{x}_T} \Big|_{(\mathbf{x}^*(T^*), \bar{\sigma})} \mathbf{p}(0) \right) \\ &\quad - \mathbf{H}^+ \cdot \left(\frac{\partial c}{\partial \mathbf{x}_T} \Big|_{(T^*, \mathbf{x}^*(T^*), y(T^*), \bar{\sigma})}^T \right), \end{aligned} \quad (21)$$

$$\mathbf{H} = \left(\frac{\partial \mathbf{g}}{\partial \mathbf{x}_T}^T \frac{\partial \mathbf{h}}{\partial \mathbf{x}_0}^T + \frac{\partial \mathbf{h}}{\partial \mathbf{x}_T}^T \right) \Big|_{(T^*, \mathbf{x}^*(T^*), \mathbf{x}^*(0), \bar{\sigma})}, \quad (22)$$

where \mathbf{H}^+ denotes the Moore–Penrose inverse of \mathbf{H} . In the case of the matrix \mathbf{H} having full rank, which is almost

always the case in passive-optimal solutions of legged systems as described in Raff et al. (2022); Rosa et al. (2023), the multiplier is uniquely reconstructed by equation (21). In this case, the constraints (1c) and (1f) are said to satisfy the *linear independence constraint qualification*.

3 Implementation

In the following, we present the numerical implementation of the first-order optimality conditions (13), (14) for the parameterized optimization problem \mathcal{P}_σ , using a single shooting approach. This involves reformulating the optimality conditions as a parameterized root-finding problem by expressing them as a zero-function. Additionally, we describe how a library of optimal gaits, represented within this parameterized zero-function, can be efficiently generated using numerical continuation methods.

3.1 Single Shooting and the Zero-Function

We begin by reformulating the boundary value problem arising from the first-order optimality conditions (13)-(14) as a single shooting problem. In this formulation, the unknown initial conditions and parameters are combined into a single decision variable

$$\boldsymbol{\chi}^T = [T \quad \mathbf{x}_0^T \quad \mathbf{p}_0^T \quad q \quad \mathbf{u}_0^T \quad \boldsymbol{\lambda}^T], \quad (23)$$

where the initial input \mathbf{u}_0 is included as an additional variable, since the DAE (13) is expressed in semi-explicit form. Starting from the initial condition $\mathbf{w}_0^T = [\mathbf{x}_0^T \ 0 \ \mathbf{p}_0^T \ q \ \mathbf{u}_0^T]$, we define the trajectory function $\boldsymbol{\varphi}_w : \mathbb{R} \times \mathbb{R}^{n_w} \times \mathbb{R}^{n_\sigma} \rightarrow \mathbb{R}^{n_w}$, where $n_w = 2n_x + 2 + n_u$, representing the solution of the autonomous DAE (13). For convenience, we use the shorthand notation $\mathbf{w}(t) := \boldsymbol{\varphi}_w(t, \mathbf{w}_0; \sigma)$ and further distinguish between the state and costate trajectories as follows:

$$\mathbf{x}(t) := \boldsymbol{\varphi}_x(t, \mathbf{w}_0; \sigma), \quad \mathbf{p}(t) := \boldsymbol{\varphi}_p(t, \mathbf{w}_0; \sigma). \quad (24)$$

The numerical computation of the trajectory $\mathbf{w}(t)$ for $t \in [0, T]$ is performed by DAE solvers as described by Brenan et al. (1995); Hairer et al. (1989). Note that numerically solving DAEs is not as straight forward as numerically integrating ODEs. In addition to our assumption of smooth dynamics, the solution quality and the choice of a suitable solver heavily depend on the index-reduction techniques applied to $\partial \mathcal{H} / \partial \mathbf{u}$.

Assumption Existence and Differentiability of Trajectories. *For any \mathbf{w}_0 and σ , the trajectory function $\boldsymbol{\varphi}_w(t, \mathbf{w}_0; \sigma)$ exists for all $t \in [0, T]$ and is differentiable with respect to σ and $\boldsymbol{\chi}$. In particular, the functions c , f , l , g , and \mathbf{h} are assumed to be continuously differentiable in σ .*

With this, we define the parameterized zero-function $\mathbf{r}_\sigma : \mathbb{R}^{N+n_\sigma} \rightarrow \mathbb{R}^N$, with $N = 2n_x + n_u + 4$, encompassing the necessary conditions (13)-(14) of the

indirect approach as:

$$\mathbf{r}_\sigma(\boldsymbol{\chi}) = \begin{bmatrix} \mathbf{r}_T(\boldsymbol{\chi}; \sigma) \\ \mathbf{r}_{\mathbf{x}T}(\boldsymbol{\chi}; \sigma) \\ q - \frac{\partial c}{\partial y_T} \Big|_{(T, \mathbf{x}(T), y(T); \sigma)} \\ \frac{\partial \mathcal{H}}{\partial \mathbf{u}} \Big|_{(\mathbf{w}(0); \sigma)} \\ \mathbf{g}(\mathbf{x}(T); \sigma) - \mathbf{x}_0 \\ \mathbf{h}(T, \mathbf{x}(T), \mathbf{x}_0; \sigma) \end{bmatrix} = \mathbf{0}, \quad (25a)$$

where

$$\begin{aligned} r_T &= \mathcal{H}(\mathbf{w}(T); \sigma) + \frac{\partial c}{\partial T} \Big|_{(T, \mathbf{x}(T), y(T); \sigma)} \\ &\quad + \boldsymbol{\lambda}^T \frac{\partial \mathbf{h}}{\partial T} \Big|_{(T, \mathbf{x}(T), \mathbf{x}_0; \sigma)}, \end{aligned} \quad (25b)$$

$$\begin{aligned} \mathbf{r}_{\mathbf{x}T} &= \frac{\partial \mathbf{g}}{\partial \mathbf{x}_T} \Big|_{(\mathbf{x}(T); \sigma)}^T \cdot \left(\mathbf{p}_0 + \frac{\partial \mathbf{h}}{\partial \mathbf{x}_0} \Big|_{(T, \mathbf{x}(T), \mathbf{x}_0; \sigma)}^T \boldsymbol{\lambda} \right) \\ &\quad - \mathbf{p}(T) + \frac{\partial c}{\partial \mathbf{x}_T} \Big|_{(T, \mathbf{x}(T), y(T); \sigma)}^T \\ &\quad + \frac{\partial \mathbf{h}}{\partial \mathbf{x}_T} \Big|_{(T, \mathbf{x}(T), y(T); \sigma)}^T \boldsymbol{\lambda}. \end{aligned} \quad (25c)$$

Furthermore, for a fixed parameter vector $\bar{\sigma}$, we define the zero-function $\mathbf{r} : \mathbb{R}^N \rightarrow \mathbb{R}^N$ such that $\mathbf{r} := \mathbf{r}_{\bar{\sigma}}$. Furthermore, imposing the differentiability assumption, we define the Jacobians:

$$\mathbf{R}(\boldsymbol{\chi}) := \frac{\partial \mathbf{r}}{\partial \boldsymbol{\chi}}, \quad \mathbf{R}(\boldsymbol{\chi}) \in \mathbb{R}^{N \times N}, \quad (26a)$$

$$\mathbf{R}_\sigma(\boldsymbol{\chi}) := \begin{bmatrix} \frac{\partial \mathbf{r}_\sigma}{\partial \boldsymbol{\chi}} & \frac{\partial \mathbf{r}_\sigma}{\partial \sigma} \end{bmatrix}, \quad \mathbf{R}_\sigma \in \mathbb{R}^{N \times (N+n_\sigma)}. \quad (26b)$$

The computation of these Jacobians is crucial for Newton-type solvers in numerical continuation methods. They are used to construct the family of gaits implicitly defined by the function (25).

3.2 Numerical Continuation

In this paper, we restrict ourselves to one-dimensional families of gaits. That is, $n_\sigma = 1$ and the function (25) implicitly defines a curve that we denote as $\mathbf{r}_\sigma^{-1}(0)$. For notational convenience, we occasionally refer to the curve as $\tilde{\mathbf{r}}^{-1}(0)$, where

$$\boldsymbol{\nu}^T := [\boldsymbol{\chi}^T \quad \sigma], \quad (27a)$$

$$\tilde{\mathbf{r}}(\boldsymbol{\nu}) := \mathbf{r}_\sigma(\boldsymbol{\chi}), \quad \tilde{\mathbf{r}} : \mathbb{R}^{N+1} \rightarrow \mathbb{R}^N, \quad (27b)$$

$$\tilde{\mathbf{R}}(\boldsymbol{\nu}) := \mathbf{R}_\sigma(\boldsymbol{\chi}), \quad \tilde{\mathbf{R}} \in \mathbb{R}^{N \times (N+1)}. \quad (27c)$$

Among the class of numerical continuation algorithms, predictor-corrector methods are well-suited to trace such an implicitly defined curve due to their strong local convergence. In this paper, we adapt the pseudo-arc length continuation method from Allgower and Georg (2003), which is outlined in Algorithm 1. This method consists of a forward Euler integration step of size $h > 0$ and direction $d \in \{-1, 1\}$, given by

$$\boldsymbol{\nu}_{\text{pred}} = \boldsymbol{\nu} + h d \boldsymbol{\tau}, \quad (28a)$$

Algorithm 1: Continuation to create 1D gait family

Input: Stationary point χ_{start} with parameter σ_{start} and desired range $[\sigma_{\text{start}}, \sigma_{\text{end}}]$; Step size $h > 0$

Output: Gait family of stationary points χ of \mathcal{P}_σ in the range $[\sigma_{\text{start}}, \sigma_{\text{end}}]$

```

1  $\nu_{\text{start}} = (\chi_{\text{start}}, \sigma_{\text{start}})$                                 /* eq. (28b) */
2 compute initial tangent vector  $\tau_{\text{start}}$           /* eq. (28d) */
3  $d \in \{-1, 1\}$                                      /* eq. (28d) */
4  $\nu \leftarrow \nu_{\text{start}}, \tau \leftarrow \tau_{\text{start}}, \sigma \leftarrow \sigma_{\text{start}}$ 
5 while  $\sigma \neq \sigma_{\text{end}}$  do
   /* predictor
    $\nu_{\text{pred}} \leftarrow \nu + dh\tau$                       /* eq. (28a) */
   compute  $\tau_{\text{pred}}$  at  $\nu_{\text{pred}}$                       /* eq. (28b) */
   /* corrector
   Newton's Method ( $\nu_{\text{pred}}, \tau_{\text{pred}}$ ):
   
$$\nu \leftarrow \nu - \left[ \begin{matrix} \tilde{R}(\nu) \\ \tau^T \end{matrix} \right]^{-1} \cdot \left[ \begin{matrix} \tilde{r}(\nu) \\ 0 \end{matrix} \right]$$

   until convergence                                         /* loop */
   return  $\{\nu_{\text{corr}} = (\chi_{\text{corr}}, \sigma_{\text{corr}}); \tau_{\text{corr}}\}$ 
12  $\nu \leftarrow \nu_{\text{corr}}, \tau \leftarrow \tau_{\text{corr}}, \sigma \leftarrow \sigma_{\text{corr}}$ 

```

where τ , referred to as the *tangent induced by $\tilde{R}(\nu)$* , is defined by

$$\tau := \left\{ \tau \in \mathbb{R}^{N+1} \middle| \begin{array}{l} \tilde{R}(\nu) \cdot \tau = 0, \\ \|\tau\|_2 = 1, \\ \det \left(\begin{bmatrix} \tilde{R}(\nu) \\ \tau^T \end{bmatrix} \right) > 0, \end{array} \right. \quad (28b)$$

and a subsequent corrector step that approximately solves the optimization problem:

$$\nu_{\text{corr}} \approx \underset{\nu \in \tilde{r}^{-1}(0)}{\operatorname{argmin}} \|\nu - \nu_{\text{pred}}\|_2, \quad (28c)$$

utilizing Newton's method. These steps are repeated until the desired family of gaits is constructed within a specified parameter range $[\sigma_{\text{start}}, \sigma_{\text{end}}]$. An initial solution χ_{start} to the zero-function (25) at the parameter σ_{start} must be known or constructed from a passive optimal gait (Section 2.4). Assuming that σ_{start} corresponds to a regular point ν_{start} (i.e., the Jacobian $\tilde{R}(\nu_{\text{start}})$ has full rank), the tangent vector (28b) is uniquely defined (Allgower and Georg 2003). However, the corresponding curve $\tilde{r}^{-1}(0)$ that passes through ν_{start} can always be traced in two directions along its tangent vector τ_{start} . To initiate the continuation process in the direction of the parameter σ_{end} , we define

$$d = \operatorname{sign}(\sigma_{\text{end}} - \sigma_{\text{start}}) \cdot \operatorname{sign}([0 \cdots 0 1] \cdot \tau_{\text{start}}). \quad (28d)$$

Algorithm 1 assumes monotonicity of the solution curve $\tilde{r}^{-1}(0)$ in the parameter $\sigma \in [\sigma_{\text{start}}, \sigma_{\text{end}}]$ to define the direction d of the curve as in equation (28d). However, in general, a curve traced via the presented pseudo-arc length continuation method may include turning points in σ as shown in Section 4.3 or bifurcation points where the one-dimensional gait family branches into higher dimensions. Consequently, it is also not guaranteed that an initial stationary point χ_{start} can be locally traced into χ_{end} corresponding to σ_{end} .

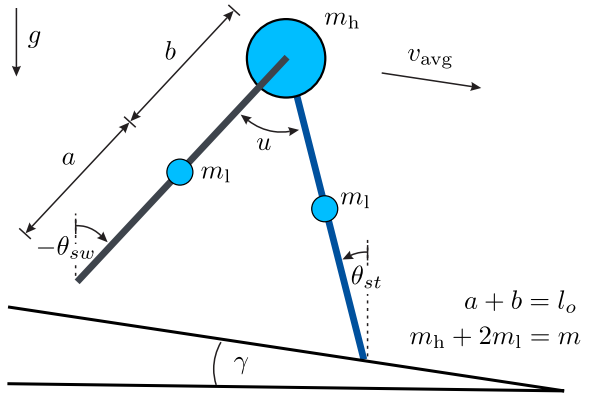


Figure 1. The compass-gait walker on a slope (γ). The robot's parameters are normalized by total mass m , gravity g and leg length l_o . Its proportions are defined as $a/b = 1$ and $m_h/m_l = 2$.

4 The Compass-Gait Walker

To demonstrate the effectiveness of the proposed methods in legged robotics, we compute optimal gaits for an underactuated compass-gait walker (Fig. 1) and compare the results with established methods based on direct trajectory optimization Wensing et al. (2024); Diehl et al. (2006); Rosa et al. (2023). Our analysis focuses on both computational efficiency and the numerical sensitivity of the different formulations. Since the indirect method does not rely on a finite parameterization of the control inputs, it serves as a reliable benchmark for assessing various input parameterizations used in direct methods. Despite the simplicity of the compass-gait walker, which has only four state variables ($n_x = 4$), it remains a widely adopted model for studying bipedal locomotion Goswami et al. (1997); Spong (1999); Asano et al. (2004); Manchester et al. (2011); Westervelt et al. (2018); Rosa and Lynch (2014); Rosa et al. (2023). Its characteristics—underactuation, non-smooth dynamics, limit cycle behavior, and the need for optimizing energy efficiency—are representative of the challenges encountered in more complex legged robots. Additionally, the compass-gait walker can passively walk down a slope driven solely by gravity g . We will use this capability to generate gait families parameterized by the slope's incline and the robot's average speed.

The model consists of a stance leg (with angle θ_{st} relative to vertical) that remains on the ground without sliding and a swing leg (with angle θ_{sw} relative to vertical) that is allowed to swing freely. During forward motion, the swing leg strikes the ground ahead of the stance leg, followed by an instantaneous switch between the swing and stance legs. Hence, the swing leg becomes the stance leg and vice versa. Both legs have a length $a + b = l_o$ with point mass m_l and are connected at the hip. The point mass m_h at the hip constitutes the main body of the biped. A single motor ($n_u = 1$) is located at the hip to provide input torques u that act between the two legs. The robot's specific proportions are provided in Figure 1, where we normalized its parameters by total mass m , gravity g , and leg length l_o . Specifically, the normalized time is defined as $t_o = \sqrt{l_o/g}$. Given its state $\mathbf{x} = [\mathbf{q} \dot{\mathbf{q}}]^T$ with configuration $\mathbf{q} = [\theta_{\text{sw}} \theta_{\text{st}}]^T$, its continuous dynamics $\mathbf{f}(\mathbf{x})$ and discrete dynamics $\mathbf{g}(\mathbf{x})$ are reported in Appendix A.2. Due to this choice of minimal

coordinates, these dynamics are independent of the slope γ . However, the slope affects the final event of both legs touching the ground:

$$e = \theta_{\text{sw}}(T) + \theta_{\text{st}}(T) + 2\gamma. \quad (29a)$$

In addition to periodicity, we require the robot to walk with a given average speed v_{avg} , which is specified within a single operating condition ($n_{\omega} = 1$):

$$\omega = 2 \sin(\theta_{\text{sw}}(T) + \gamma) - v_{\text{avg}}T. \quad (29b)$$

Equations (29a) and (29b) constitute the equality constraint $\mathbf{h}(T, \mathbf{x}(T), \mathbf{x}(0); \boldsymbol{\sigma}) = \mathbf{0}$ within the parameterized optimization problem $\mathcal{P}_{\boldsymbol{\sigma}}$, where $\boldsymbol{\sigma}^T = [\gamma \ v_{\text{avg}}]$. The objective in this example is to minimize the cost of transport, defined as

$$c = \frac{y(T)}{mg\Delta x} \quad \left| \quad \dot{y} = \underbrace{\frac{k}{2} u^2}_{=l(\mathbf{x}, u)}, \quad \Delta x = v_{\text{avg}}T, \quad (30) \right.$$

where the constant $k = (m\sqrt{gl_o})^{-1}$ relates to the speed-torque gradient of a DC-motor. Note that the traveled distance Δx is typically strictly positive and bounded to ensure meaningful gaits with forward motion. As a result, the cost reaches its minimum value of zero only at passive optimal gaits, where $u \equiv 0$.

Remark 4.1. *With the stage cost defined as $l = k/2 u^2$, the reconstruction of Lagrange multipliers at passive optimal gaits (Section 2.4) becomes straightforward, as the vector $\tilde{\mathbf{b}}$ from equation (19c) vanishes. Consequently, from equation (20), the costate \mathbf{p} is zero at all times ($\mathbf{p} \equiv \mathbf{0}$). By inspection of equation (21), the Lagrange multiplier $\boldsymbol{\lambda}$ is also zero ($\boldsymbol{\lambda} = \mathbf{0}$). The remaining scalar costate q is reconstructed using equation (16), yielding $q = (mgv_{\text{avg}}T^*)^{-1}$.*

In the following, we leverage the passive optimal gaits of the compass-gait walker to initialize Algorithm 1, generating optimal families of gaits within the parameterized optimization problem $\mathcal{P}_{\boldsymbol{\sigma}}$ (Section 4.1). Additionally, this workflow allows for a performance and accuracy comparison between the indirect and direct methods (Section 4.2). This comparison is extended to gait families that do not include passive gaits (Section 4.3).

Algorithm 1 is implemented in MATLAB with a tolerance of 10^{-8} for evaluating $\tilde{\mathbf{r}} = \mathbf{0}$. We use MATLAB's variable step-size integrator `ode15s`, with relative and absolute tolerances of 10^{-9} and 10^{-10} , respectively, to solve the DAEs within $\tilde{\mathbf{r}}$. To ensure a fair comparison, the same settings are applied for solving the ODEs in the direct method. For simplicity, the Jacobians $\tilde{\mathbf{R}}$ are approximated using forward finite differences with a step size of 10^{-9} . The corresponding code is available on GitHub*.

4.1 From Passive to Level Ground Walking

To demonstrate the exploratory potential of the indirect approach combined with numerical continuation, an initial library of gaits is generated based on the passive gaits of the compass-gait walker, similar to the work in Rosa et al. (2023). As detailed in Rosa and Lynch (2014), passive gaits can be systematically derived from standing still

(equilibrium) using pseudo-arc length continuation, with the slope γ varied as well. As shown in Fig. 2a, two distinct curves of passive gaits emerge from the standstill: one with a shorter period (T_{short}) and another with a longer period (T_{long}), corresponding to the swing leg taking a shorter or longer time to strike the ground, respectively. To generate a 1D family of optimal gaits on a varying slope, we employ the scalar continuation parameter $\sigma := \gamma$, while constraining the average speed to $v_{\text{avg}} = 0.1\sqrt{gl_o}$. We initialize Algorithm 1 with a passive gait at slope γ_l , which corresponds to the longer period (T_{long}) at $v_{\text{avg}} = 0.1\sqrt{gl_o}$. This passive gait serves as the optimal passive solution, represented by the tuple $(T_l^*, \mathbf{x}_l^*(\cdot), u_l^*(\cdot))$, with zero input $u_l^* \equiv 0$ and cost $c = 0$ for the parameterized optimization problem \mathcal{P}_{γ} .

As noted in Remark 4.1, the reconstruction of the costates and Lagrange multipliers is straightforward. Thus, Algorithm 1 is initialized with

$$\chi_{\text{start}} = \begin{bmatrix} T_{\text{start}} \\ \mathbf{x}_{0,\text{start}} \\ \mathbf{p}_{0,\text{start}} \\ q_{\text{start}} \\ u_{0,\text{start}} \\ \boldsymbol{\lambda}_{\text{start}} \end{bmatrix} = \begin{bmatrix} T_l^* \\ \mathbf{x}_l^*(0) \\ \mathbf{0} \\ (mgv_{\text{avg}}T_l^*)^{-1} \\ 0 \\ \mathbf{0} \end{bmatrix}, \quad (31a)$$

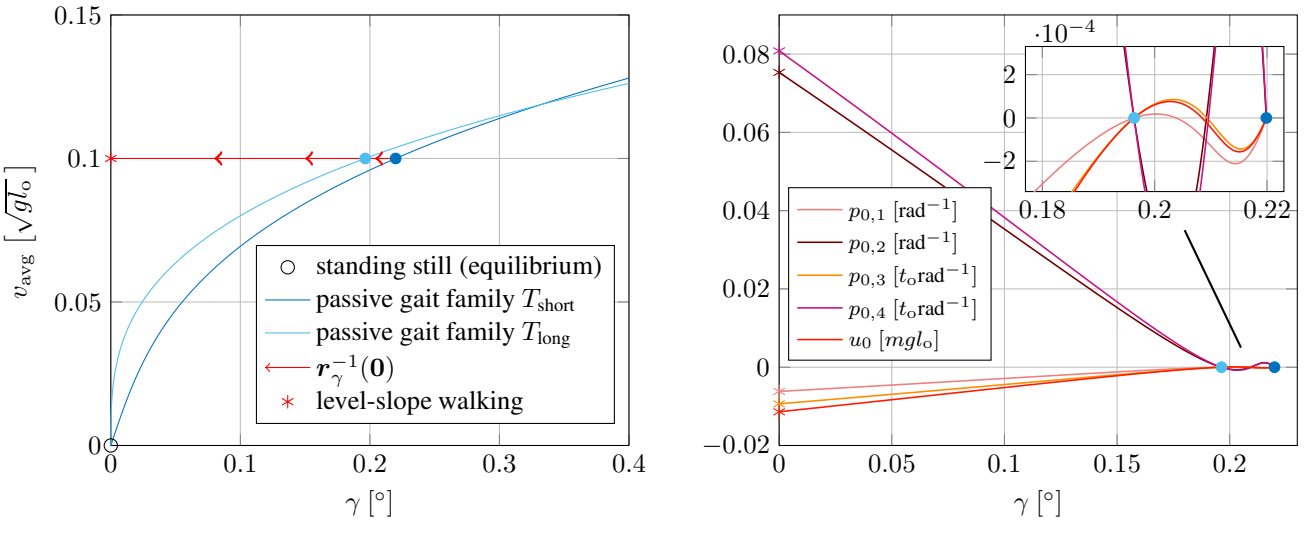
$$\sigma_{\text{start}} = \gamma_l, \quad (31b)$$

where $v_{\text{avg}} = 0.1\sqrt{gl_o}$ is fixed throughout the algorithm. To generate a gait family that includes level-ground walking, the desired range of the slope parameter is set to $[\sigma_{\text{start}}, \sigma_{\text{end}}] = [\gamma_l, 0^\circ]$. Figure 2a shows a projection of the gait family curve $\mathbf{r}_{\gamma}^{-1}(0)$, depicted in red, as the output of Algorithm 1. The red curve also indicates an intersection with the other passive gait family, characterized by a shorter period (T_{short}). In Figure 2b, we further illustrate how the initial costates \mathbf{p}_0 and input u_0 vanish at those slopes γ where a passive gait exists, corresponding to an average speed of $v_{\text{avg}} = 0.1\sqrt{gl_o}$.

4.2 Comparison to the Direct Method

Building on the gait family $\mathbf{r}_{\gamma}^{-1}(0)$ computed in the previous section, we perform a comparison between the indirect method and the direct method. The direct method, combined with a variable step-size shooting approach (MATLAB's `ode15s`), requires a parameterization $\boldsymbol{\xi} \in \mathbb{R}^{n_{\xi}}$, with $n_{\xi} > 1$, of the input space, where the control input is defined as $\mathbf{u} := \hat{\mathbf{u}}(t, \boldsymbol{\xi})$. This readily allows to numerically solve the differential equation (1b) and yields the flow $\dot{\mathbf{x}}(t) := \varphi_{\mathbf{x}}(t, \mathbf{x}_0, \boldsymbol{\xi})$. We implement and compare a cubic B-spline and a Bézier curve implementation for varying n_{ξ} , which are common input parameterizations that provide high accuracy for a small number of parameters n_{ξ} (Lin et al. 2014). A detailed description of the input parameterizations and our implementation of the direct method is provided in Appendix A.3. By transcribing the input space of problem $\mathcal{P}_{\boldsymbol{\sigma}}$ with $\mathbf{u} := \hat{\mathbf{u}}(t, \boldsymbol{\xi})$, we pose the direct shooting problem as an implicit function, similar to the

*github.com/raffmax/IndirectMethod



(a) The continuation process towards level-ground walking, crossing two passive gaits.

(b) The evolution of initial costates p_0 and input u_0 within the implicit curve $r_\gamma^{-1}(0)$. At passive gaits ($u \equiv 0$), the costates vanish ($p \equiv 0$).

Figure 2. Projections of the implicit curve $r_\gamma^{-1}(0)$, computed using Algorithm 1 with the continuation parameter $\sigma := \gamma$. The curve corresponds to a fixed average speed of $v_{\text{avg}} = 0.1 \sqrt{g l_o}$ and originates from the passive gait family with the shorter period time T_{short} . As the curve progresses towards level slope at $\gamma = 0^\circ$ (marked by *), it intersects the passive gait family with the longer period time T_{long} . The filled circles indicate points where the passive and optimal gaits coincide.

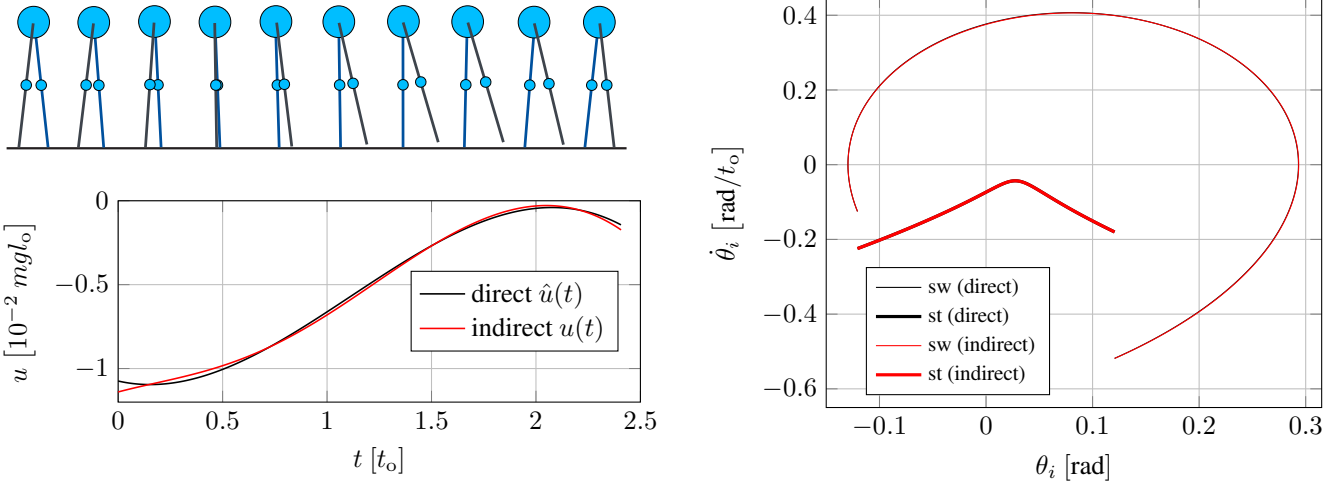


Figure 3. Visualization of an optimal walking gait at an average velocity of $v_{\text{avg}} = 0.1 \sqrt{g l_o}$ on a level slope ($\gamma = 0^\circ$). The keyframes depict the compass-gait walker, while the input and state trajectories (swing leg "sw" and stance leg "st") are shown for both the indirect (red) and direct (black) shooting methods. The black curves, representing the direct method, correspond to an input parameterization using a single cubic B-spline with $n_\xi = 4$.

parameterized indirect method in equation (25). Hence, the zero-function $\hat{r}_\sigma : \mathbb{R}^{\hat{N}+n_\sigma} \rightarrow \mathbb{R}^{\hat{N}}$ of the direct method, with $\hat{N} = 2n_x + n_\xi + 3$, is defined as

$$\hat{r}_\sigma(\hat{\chi}) = \begin{bmatrix} \frac{\partial \hat{e}}{\partial \hat{s}}|_{(\hat{s}, \sigma)}^T + \frac{\partial \hat{h}}{\partial \hat{s}}|_{(\hat{s}, \sigma)}^T \hat{\lambda} \\ \hat{h}|_{(\hat{s}, \sigma)} \end{bmatrix} = \mathbf{0}, \quad (32a)$$

$$\hat{\chi}^T = \begin{bmatrix} [T \quad \mathbf{x}_0^T \quad \boldsymbol{\xi}^T] \\ =: \hat{s}^T & \hat{\lambda}^T \end{bmatrix}, \quad (32b)$$

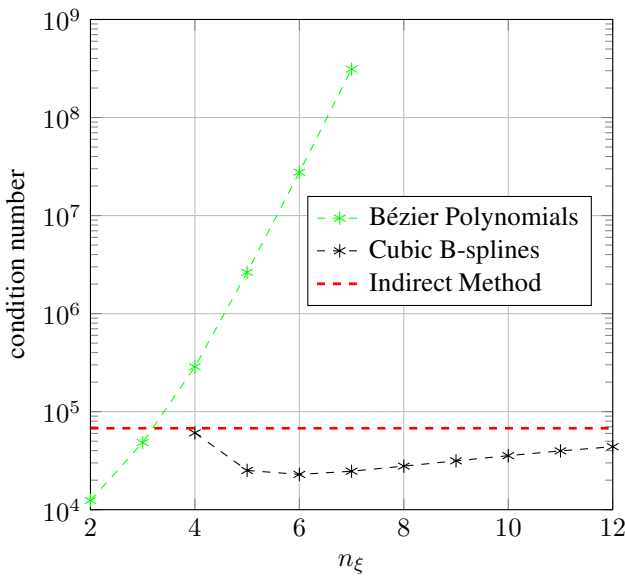
where

$$\hat{e}(\hat{s}, \sigma) = c(T, \mathbf{x}(T), y(T); \sigma), \quad (32c)$$

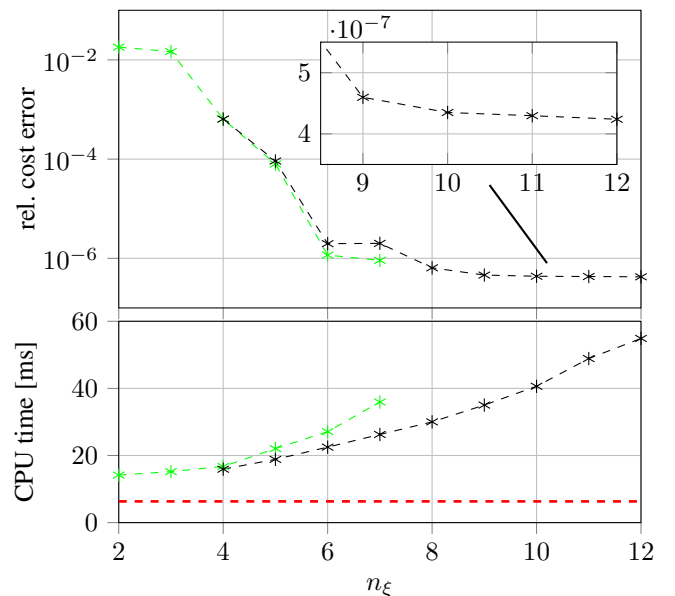
$$\hat{h}(\hat{s}, \sigma) = \begin{bmatrix} \mathbf{g}(\hat{\mathbf{x}}(T)) - \mathbf{x}_0 \\ \mathbf{h}(T, \hat{\mathbf{x}}(T), \mathbf{x}_0; \sigma) \end{bmatrix}, \quad (32d)$$

and $\hat{\lambda} \in \mathbb{R}^{n_x+2}$ is the associated Lagrange multiplier to the constraint (32d). Similar to the indirect case, when the parameters σ are fixed, we refer to the zero function (32) as $\hat{r} \in \mathbb{R}^{\hat{N}} \rightarrow \mathbb{R}^{\hat{N}}$. And likewise, its respective Jacobians are denoted as $\hat{\mathbf{R}}_\sigma \in \mathbb{R}^{\hat{N} \times \hat{N}+n_\sigma}$ and $\hat{\mathbf{R}} \in \mathbb{R}^{\hat{N} \times \hat{N}}$.

In accordance with Rosa et al. (2023), we utilize the direct shooting implementation of the zero-function 32 and Algorithm 1 to generate a family of gaits $\hat{r}_\gamma^{-1}(0)$, which includes both passive gaits and a level-ground walking gait in the parameter range $[\sigma_{\text{start}}, \sigma_{\text{end}}] = [\gamma_1, 0^\circ]$. As in the implicit shooting method described in Section 4.1, we define the scalar continuation parameter as $\sigma := \gamma$, while constraining the average speed to $v_{\text{avg}} = 0.1 \sqrt{g l_o}$.



(a) Condition numbers of the indirect Jacobian ($\hat{\mathbf{R}}$) and direct Jacobian ($\hat{\mathbf{R}}$). The direct method using Bézier polynomials fails to converge for $n_\xi > 7$ due to high sensitivity in ξ within the shooting problem.



(b) Relative error $\frac{\hat{c} - c}{c}$ in the optimal cost between the direct method (\hat{c}) and the indirect method (c), along with the average CPU time over 1000 evaluations of the indirect function \hat{r} and the direct function r .

Figure 4. Comparison of the direct (\hat{r}) and indirect (r) approaches in a MATLAB implementation on an Intel Core i5-8500 CPU @ 3.00GHz with 8GB RAM. In the direct method, the input space is parameterized with either Bézier polynomials or cubic B-Splines, introducing n_ξ variables. The data in a) and b) corresponds to walking on a level slope ($\gamma = 0^\circ$) at an average speed of $v_{\text{avg}} = 0.1\sqrt{gl_0}$. The corresponding (locally) optimal gaits were generated via continuation from a passive gait using Algorithm 1, as shown in Fig. 2.

Figures 3 and 4 compare the direct (\hat{r}) and indirect (r) shooting methods for a locally optimal gait at level slope ($\gamma = 0^\circ$) and average speed $v_{\text{avg}} = 0.1\sqrt{gl_0}$.

To analyze and contrast the region of convergence, we compute the condition numbers of \mathbf{R} and $\hat{\mathbf{R}}$ for varying numbers of input parameters n_ξ (Fig. 4a). While the condition number of the indirect method remains constant, as it is independent of the input parameterization, the condition number of $\hat{\mathbf{R}}$ varies with n_ξ . The control input parameterization using Bézier polynomials becomes highly sensitive to parameter variations as n_ξ increases. This sensitivity arises from the global nature of this parameterization, where adjusting a single parameter ξ_i in the vector ξ affects the entire shape of the input curve $\hat{u}(t, \xi)$. As a result, for $n_\xi > 7$, Algorithm 1 stalled at certain points in traversing $\hat{r}_\gamma^{-1}(0)$, where Newton's method failed to converge due to the high sensitivities and the use of forward finite differences in computing $\hat{\mathbf{R}}_\gamma$.

In contrast, the cubic B-spline parameterization introduces $n_\xi - 3$ equidistant segments in the input space, which are locally decoupled. Thus, a variation in a single parameter ξ_i only locally affects the input curve $\hat{u}(t, \xi)$. This allows for arbitrarily large parameterizations without a blow-up in the condition number, as illustrated in Fig. 4a. Therefore, as the accuracy of approximating the control input space increases, cubic B-splines are much better suited. This is also evident in Fig. 4b, which shows the relative cost error of direct shooting ($\hat{c} - c$) compared to the indirect cost (c). Note that the cost value \hat{c} of the cubic B-spline parameterization approaches the indirect cost value c as n_ξ increases, although it remains inferior. It is also worth noting that Bézier polynomials and cubic B-splines yield the same cost value

at $n_\xi = 4$ since both describe a cubic curve. However, the CPU time required to evaluate \hat{r} for these parameterizations differs slightly, as cubic B-splines are more efficiently computed in a recursive manner (Appendix A.3.1). This plot of CPU times also highlights that indirect shooting can be significantly faster than direct shooting when n_ξ becomes large.

There is, of course, considerable room for improving efficiency, as the current implementation is in MATLAB. In addition to optimizing runtime by transitioning to a more efficient programming language such as Julia or C++, there is potential for accelerating both the direct and indirect shooting approaches. Specifically, there are alternative approaches for computing the first-order condition within equation (32a) in the direct method, as detailed in Appendix A.3.2. Likewise, the indirect shooting approach can be significantly accelerated by eliminating the input variable u_0 from χ . Often, the control input u can be explicitly expressed as a function of x , p , and q by utilizing $\partial\mathcal{H}/\partial u = 0$. With a stage cost $l = k/2u^2$ and the input-affine dynamics of the compass-gait walker, the input takes the form:

$$u = -\frac{1}{kq} \frac{\partial f}{\partial u} \bigg|_{x(t)}^T \cdot p(t).$$

By eliminating the variable u_0 , this step transforms the DAE into an ODE in x and p , which can generally be solved more quickly. This transformation also allows for the application of variable step-size symplectic integrators (Hairer 1997), which effectively exploit the Hamiltonian structure. Such integrators enhance conservation properties throughout the simulation and can be particularly beneficial in addressing

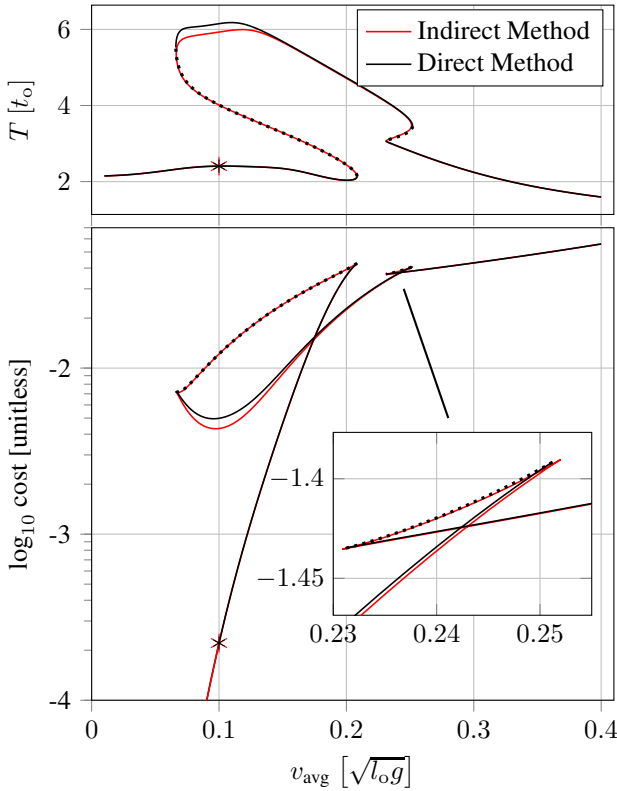


Figure 5. Projections of the implicit curves derived from the indirect method $r_{v_{\text{avg}}}^{-1}(\mathbf{0})$ and the direct method $\hat{r}_{v_{\text{avg}}}^{-1}(\mathbf{0})$, both computed using Algorithm 1 with the continuation parameter $\sigma = v_{\text{avg}}$. These curves represent level-slope walking ($\gamma = 0^\circ$) and originate from an optimal gait at $v_{\text{avg}} = 0.1 \sqrt{g t_o}$ (denoted by *). The indirect method consistently yields gaits with lower costs, whereas the direct method (utilizing cubic B-splines with $n_\xi = 4$) can distinguish local minima (solid black line) from saddle points (dotted black line) by applying second-order optimality conditions.

shooting problems when the period T is large. However, these refinements, including a detailed examination of the computational efficiency trade-offs between direct and indirect shooting methods, are beyond the scope of this work and will be addressed in future research.

4.3 Generation of Additional Gait Families

In addition to the previous sections, we further demonstrate the versatility and practical applicability of the proposed methods in legged locomotion by generating an additional family of optimal gaits that do not directly stem from passive dynamics. Specifically, we use the previously computed locally optimal gait at level slope ($\gamma = 0^\circ$) and average speed $v_{\text{avg}} = 0.1 \sqrt{g t_o}$ to initialize Algorithm 1 for the generation of a family of level walking gaits $r_{v_{\text{avg}}}^{-1}(\mathbf{0})$. Unlike earlier sections where we varied the slope, we now fix the slope at $\gamma = 0^\circ$ and vary the speed, using it as our continuation parameter $\sigma = v_{\text{avg}}$. This approach underscores the method’s ability to adapt to different operating conditions, extending its relevance to practical robotic systems.

As shown in Fig. 5, we generate the gait family (red curve) by running Algorithm 1 twice, with $\sigma_{\text{end}} = 0.01 \sqrt{g t_o}$ and $\sigma_{\text{end}} = 0.4 \sqrt{g t_o}$. In the latter case, tracing $r_{v_{\text{avg}}}^{-1}(\mathbf{0})$

involves four turning points in v_{avg} , resulting in multiple stationary gaits for certain ranges of v_{avg} . Since we do not impose second-order conditions, we cannot distinguish between locally optimal points and saddle points using the indirect method. Working out second-order variational theory becomes cumbersome even for small subclasses of periodic optimization problems of \mathcal{P} (Speyer and Evans 1984). Among other requirements, deriving conditions for weak local minima involves showing the existence of particular solutions to Riccati differential equations and analyzing distinct properties of the Monodromy matrix of the underlying DAE/ODE.

While deriving second-order conditions for \mathcal{P} is out of scope for this work, we leverage the direct method for comparison, as these conditions are more accessible (see Appendix A.3.3). The black curve in Fig. 5 shows projections from the direct shooting approach (points in $\hat{r}_{v_{\text{avg}}}^{-1}$) using a single cubic B-spline ($n_\xi = 4$). Solid lines indicate strict local minimizers, while dashed lines correspond to families of saddle points. When traversing the curve $\hat{r}_{v_{\text{avg}}}^{-1}$, the switch between minimizer and saddle point always occurs at turning points in v_{avg} .

Furthermore, examining the cost plot in Fig. 5, we can distinguish between good and bad local minima. Notably, similar to Fig. 4b, the indirect method consistently yields a lower cost value. This is due to the input space parametrization in the direct method, which can only approximate the true optimal solution, whereas the indirect method is more flexible, utilizing an adaptive step-size DAE solver.

5 Conclusion & Discussion

In this work, we have provided advancements in periodic trajectory optimization for systems with hybrid dynamics, particularly in the context of legged locomotion. Our key contributions include the formalization of a general trajectory optimization problem that extends first-order necessary conditions to a wider class of cost functions and periodic hybrid systems. We introduced a framework for generating and analyzing families of optimal gaits using the indirect shooting method, coupled with numerical continuation techniques. A major feature of this approach is the initialization of gait libraries with optimal periodic motions that exhibit vanishing actuation (passive gaits), for which Lagrange multipliers and costates can be effectively reconstructed. By comparing the indirect and direct shooting methods on the compass-gait walker, we demonstrated that the indirect method provides superior accuracy in generating optimal solutions, while addressing the inherent challenges of input space parameterization more effectively.

Despite these advancements, several important areas remain open for further research. While our results suggest that the indirect shooting method offers faster function evaluations compared to the direct method in the context of the compass-gait walker, a more detailed analysis of the numerical complexity involved in the indirect method is necessary. Such an analysis would offer a clearer understanding of the computational trade-offs between indirect and direct shooting approaches and could lead to broader, more definitive conclusions about their relative

efficiency as system complexity increases across various legged and hybrid dynamical systems.

Furthermore, the first-order necessary conditions derived in this work are currently tailored to simple hybrid systems, characterized by a single continuous and a single discrete dynamic map. A critical direction for future research involves extending these conditions to address more complex locomotion patterns, such as running or walking with a double support phase, where foot lift-off and touch-down do not occur simultaneously. Such extensions would require incorporating kinetic events (such as a foot leaving the ground when ground reaction forces reach zero) into the event definitions. Currently, our event functions are solely defined kinematically or by time, but this extension would necessitate incorporating actuation inputs (u) into the definition of the event function. Moreover, the introduction of multiple hybrid phases would convert the current two-point boundary problem into a multi-point boundary problem. This transformation could be effectively addressed using a multiple shooting approach, where the initial shooting conditions align with the image of the discrete (reset) maps.

Another important future direction involves the integration of inequality path constraints into the indirect method. Addressing such constraints (e.g., joint limits or actuator torque limits) would require dividing the time domain into subarcs where these inequality constraints are either active or inactive, as described by Betts (2010). This could also be addressed by introducing a multiple shooting scheme. However, a major challenge here is the unknown number and order of these subarcs, which complicates the application of variable step-size shooting methods. Developing strategies to handle this complexity would significantly enhance the versatility of the indirect method and broaden its applicability to more complex, real-world systems where inequality constraints are critical.

While there is room for further refinement and extension of the indirect method for periodic trajectory optimization, this work underscores advantages of the indirect approach over traditional direct methods, particularly in terms of accuracy. The methodologies and insights presented in this paper mark a significant step forward in the application of indirect methods to the challenging and dynamic field of legged robotic systems.

Acknowledgements

This work was funded by the Deutsche Forschungsgemeinschaft (DFG, German Research Foundation) – 501862165. It was further supported through the International Max Planck Research School for Intelligent Systems (IMPRS-IS) for Maximilian Raff.

References

- E. L. Allgower and K. Georg. *Introduction to numerical continuation methods*. Society for Industrial and Applied Mathematics, jan 2003. doi: 10.1137/1.9780898719154.
- A. D. Ames. *A categorical theory of hybrid systems*. Phd thesis, Citeseer, 2006. URL <http://ames.caltech.edu/A%20categorical%20theory.pdf>.
- F. Asano, M. Yamakita, N. Kamamichi, and Z.-W. Luo. A novel gait generation for biped walking robots based on mechanical energy constraint. *IEEE Transactions on Robotics and Automation*, 20(3):565–573, June 2004. ISSN 1042-296X. doi: 10.1109/tra.2004.824685.
- J. T. Betts. *Practical methods for optimal control and estimation using nonlinear programming*. Society for Industrial and Applied Mathematics, Jan. 2010. ISBN 9780898718577. doi: 10.1137/1.9780898718577.
- K. E. Brenan, S. L. Campbell, and L. R. Petzold. *Numerical solution of initial-value problems in differential-algebraic equations*. Society for Industrial and Applied Mathematics, Jan. 1995. ISBN 9781611971224. doi: 10.1137/1.9781611971224.
- P. H. Channon, S. H. Hopkins, and D. T. Pham. A variational approach to the optimization of gait for a bipedal robot. *Proceedings of the Institution of Mechanical Engineers, Part C: Journal of Mechanical Engineering Science*, 210(2):177–186, Mar. 1996. ISSN 2041-2983. doi: 10.1243/pime_proc-1996_210_184_02.
- F. Colonius. *Optimal periodic control*. Springer Berlin Heidelberg, 1988. ISBN 9783540391708. doi: 10.1007/bfb0077931.
- R. P. Dickinson and R. J. Gelinas. Sensitivity analysis of ordinary differential equation systems—a direct method. *Journal of Computational Physics*, 21(2):123–143, jun 1976. doi: 10.1016/0021-9991(76)90007-3.
- M. Diehl, H. Bock, H. Diedam, and P.-B. Wieber. *Fast direct multiple shooting algorithms for optimal robot control*, pages 65–93. Springer Berlin Heidelberg, 2006. ISBN 9783540361183. doi: 10.1007/978-3-540-36119-0_4.
- E. Gilbert and D. Lyons. The improvement of aircraft specific range by periodic control. In *Guidance and Control Conference*. American Institute of Aeronautics and Astronautics, Aug. 1981. doi: 10.2514/6.1981-1748.
- A. Goswami, B. Espiau, and A. Keramane. Limit cycles in a passive compass gait biped and passivity-mimicking control laws. *Autonomous Robots*, 4(3):273–286, 1997. ISSN 0929-5593. doi: 10.1023/a:1008844026298.
- S. Gros and M. Diehl. Numerical optimal control. Lecture Notes Draft, 2022. URL <https://www.syscop.de/files/2020ss/NOC/book-NOCSE.pdf>.
- E. Hairer. Variable time step integration with symplectic methods. *Applied Numerical Mathematics*, 25(2–3):219–227, Nov. 1997. ISSN 0168-9274. doi: 10.1016/s0168-9274(97)00061-5.
- E. Hairer, M. Roche, and C. Lubich. *The numerical solution of differential-algebraic systems by Runge-Kutta methods*. Springer Berlin Heidelberg, 1989. ISBN 9783540468325. doi: 10.1007/bfb0093947.
- F. J. M. Horn and R. C. Lin. Periodic processes: A variational approach. *Industrial and Engineering Chemistry Process Design and Development*, 6(1):21–30, Jan. 1967. ISSN 1541-5716. doi: 10.1021/i260021a005.
- B. Houska and B. Chachuat. Branch-and-lift algorithm for deterministic global optimization in nonlinear optimal control. *Journal of Optimization Theory and Applications*, 162(1):208–248, Sept. 2013. ISSN 1573-2878. doi: 10.1007/s10597-013-0426-1.
- A. Isidori. *Nonlinear control systems*. Springer London, 1995. ISBN 9781846286155. doi: 10.1007/978-1-84628-615-5.

D. Kalman. Leveling with lagrange: An alternate view of constrained optimization. *Mathematics Magazine*, 82(3):186–196, June 2009. ISSN 1930-0980. doi: 10.1080/0025570x.2009.11953617.

M. Kelly. An introduction to trajectory optimization: How to do your own direct collocation. *SIAM Review*, 59(4):849–904, Jan. 2017. ISSN 1095-7200. doi: 10.1137/16m1062569.

D. Liberzon. *Calculus of variations and optimal control theory: A concise introduction*. Princeton University Press, Dec. 2011. ISBN 9780691151878. doi: 10.2307/j.ctvcm4g0s.

Q. Lin, R. Loxton, and K. Lay Teo. The control parameterization method for nonlinear optimal control: A survey. *Journal of Industrial & Management Optimization*, 10(1):275–309, 2014. ISSN 1553-166X. doi: 10.3934/jimo.2014.10.275.

D. G. Luenberger. *Optimization by vector space methods*. John Wiley & Sons, 1997.

D. G. Luenberger and Y. Ye. *Linear and nonlinear programming*. Springer International Publishing, 2021. ISBN 9783030854508. doi: 10.1007/978-3-030-85450-8.

I. R. Manchester, M. M. Tobenkin, M. Levashov, and R. Tedrake. Regions of attraction for hybrid limit cycles of walking robots. *IFAC Proceedings Volumes*, 44(1):5801–5806, jan 2011. doi: 10.3182/20110828-6-it-1002.03069.

L. Piegl and W. Tiller. *The NURBS book*. Springer Berlin Heidelberg, 1997. ISBN 9783642592232. doi: 10.1007/978-3-642-59223-2.

L. Pontryagin. *Mathematical theory of optimal processes*. Routledge, May 1987. ISBN 9780203749319. doi: 10.1201/9780203749319.

M. Raff, N. Rosa, and C. D. Remy. Generating families of optimally actuated gaits from a legged system’s energetically conservative dynamics. In 2022 IEEE/RSJ International Conference on Intelligent Robots and Systems (IROS). IEEE, Oct. 2022. doi: 10.1109/iros47612.2022.9981693.

J. Reher and A. D. Ames. Inverse dynamics control of compliant hybrid zero dynamic walking. In 2021 IEEE International Conference on Robotics and Automation (ICRA). IEEE, May 2021. doi: 10.1109/icra48506.2021.9560906.

N. Rosa and K. M. Lynch. Extending equilibria to periodic orbits for walkers using continuation methods. In 2014 IEEE/RSJ International Conference on Intelligent Robots and Systems. IEEE, sep 2014. doi: 10.1109/iros.2014.6943076.

N. Rosa, B. Katamish, M. Raff, and C. D. Remy. An approach for generating families of energetically optimal gaits from passive dynamic walking gaits. In 2023 IEEE/RSJ International Conference on Intelligent Robots and Systems (IROS). IEEE, Oct. 2023. doi: 10.1109/iros55552.2023.10342322.

I. M. Ross. A direct shooting method is equivalent to an indirect method, 2020. URL <https://arxiv.org/abs/2003.02418>.

B. Sengupta, K. Friston, and W. Penny. Efficient gradient computation for dynamical models. *NeuroImage*, 98:521–527, Sept. 2014. ISSN 1053-8119. doi: 10.1016/j.neuroimage.2014.04.040.

J. Speyer and R. Evans. A second variational theory for optimal periodic processes. *IEEE Transactions on Automatic Control*, 29(2):138–148, Feb. 1984. ISSN 0018-9286. doi: 10.1109/tac.1984.1103482.

J. L. Speyer. Periodic optimal flight. *Journal of Guidance, Control, and Dynamics*, 19(4):745–755, July 1996. ISSN 1533-3884. doi: 10.2514/3.21695.

M. W. Spong. Passivity based control of the compass gait biped. *IFAC Proceedings Volumes*, 32(2):506–510, July 1999. ISSN 1474-6670. doi: 10.1016/s1474-6670(17)56086-3.

O. von Stryk and R. Bulirsch. Direct and indirect methods for trajectory optimization. *Annals of Operations Research*, 37(1):357–373, Dec. 1992. ISSN 1572-9338. doi: 10.1007/bf02071065.

P. M. Wensing, M. Posa, Y. Hu, A. Escande, N. Mansard, and A. D. Prete. Optimization-based control for dynamic legged robots. *IEEE Transactions on Robotics*, 40:43–63, 2024. ISSN 1941-0468. doi: 10.1109/tro.2023.3324580.

E. R. Westervelt, J. W. Grizzle, C. Chevallereau, J. H. Choi, and B. Morris. *Feedback control of dynamic bipedal robot locomotion*. CRC Press, oct 2018. doi: 10.1201/9781420053739.

A Appendix

A.1 First-Order Variation

The first-order variation defined in equation (8) is executed in its three components (4). This is done in equations (33)–(35), where we used the Leibniz integral rule in equation (35a) and integration by parts in equation (35b). Taking the sum of equations (33)–(35) with additional grouping of terms yields equation (9a).

A.2 Dynamics of the Compass-Gait Walker

With the minimal coordinates $\mathbf{q} = [\theta_{\text{sw}} \ \theta_{\text{st}}]^T$, the auxiliary angle $\alpha(\mathbf{q}) = \theta_{\text{st}} - \theta_{\text{sw}}$ and the leg length $l_o = a + b$, we define the continuous dynamics as

$$\mathbf{M}(\mathbf{q})\ddot{\mathbf{q}} + \mathbf{C}(\mathbf{q}, \dot{\mathbf{q}})\dot{\mathbf{q}} + \mathbf{G}(\mathbf{q}) = \mathbf{B}u, \quad (36a)$$

where,

$$\mathbf{M} = \begin{bmatrix} m_h b^2 & -m_l l_o b \cos(\alpha) \\ -m_l l_o b \cos(\alpha) & (m_h + m_l) l_o^2 + m a^2 \end{bmatrix}, \quad (36b)$$

$$\mathbf{C} = \begin{bmatrix} 0 & m_l l_o b \sin(\alpha) \dot{\theta}_{\text{st}} \\ -m_l l_o b \sin(\alpha) \dot{\theta}_{\text{sw}} & 0 \end{bmatrix}, \quad (36c)$$

$$\mathbf{G} = \begin{bmatrix} m_l b g \sin(\theta_{\text{sw}}) \\ -(m_h l_o + m_l a + m_l l_o) g \sin(\theta_{\text{st}}) \end{bmatrix}, \quad (36d)$$

$$\mathbf{B} = \begin{bmatrix} -1 \\ 1 \end{bmatrix}. \quad (36e)$$

Hence, with the state $\mathbf{x}^T = [\mathbf{q}^T \ \dot{\mathbf{q}}^T]$, the vector field takes the form

$$\mathbf{f}(\mathbf{x}, u) = \begin{bmatrix} \dot{\mathbf{q}} \\ \mathbf{M}(\mathbf{q})^{-1}(\mathbf{B}u - \mathbf{C}(\mathbf{q}, \dot{\mathbf{q}})\dot{\mathbf{q}} - \mathbf{G}(\mathbf{q})) \end{bmatrix}. \quad (37)$$

The equations for the collision of the swing-leg with the ground are derived by conservation of angular momentum:

$$\mathbf{Q}^+(\mathbf{q})\dot{\mathbf{q}}^+ = \mathbf{Q}^-(\mathbf{q})\dot{\mathbf{q}}^-, \quad (38a)$$

$$\frac{dL_1}{d\varepsilon} \Big|_{\varepsilon=0} = \frac{dc}{d\varepsilon} \left(\tilde{T}, \mathbf{z}^*(\tilde{T}) + \varepsilon \cdot \delta \mathbf{z}(\tilde{T}) \right) \Big|_{\varepsilon=0} + \frac{d}{d\varepsilon} \left(\tilde{\boldsymbol{\lambda}}^T \mathbf{h}(\tilde{T}, \mathbf{x}^*(\tilde{T}) + \varepsilon \delta \mathbf{x}(\tilde{T}), \mathbf{x}^*(0) + \varepsilon \delta \mathbf{x}(0)) \right) \Big|_{\varepsilon=0} \quad (33a)$$

$$\begin{aligned} &= \left[\frac{\partial c}{\partial T} \Big|_* + \frac{\partial c}{\partial \mathbf{z}_T} \Big|_* \dot{\mathbf{z}}^*(T^*) + \boldsymbol{\lambda}^{*T} \left(\frac{\partial \mathbf{h}}{\partial T} \Big|_* + \frac{\partial \mathbf{h}}{\partial \mathbf{x}_T} \Big|_* \dot{\mathbf{x}}^*(T^*) \right) \right] \delta T + \delta \boldsymbol{\lambda}^T \mathbf{h}|_* \\ &+ \frac{\partial c}{\partial y_T} \Big|_* \delta y(T^*) + \left[\frac{\partial c}{\partial \mathbf{x}_T} \Big|_* + \boldsymbol{\lambda}^{*T} \frac{\partial \mathbf{h}}{\partial \mathbf{x}_T} \Big|_* \right] \delta \mathbf{x}(T^*) + \boldsymbol{\lambda}^{*T} \frac{\partial \mathbf{h}}{\partial \mathbf{x}_0} \Big|_* \delta \mathbf{x}(0), \end{aligned} \quad (33b)$$

$$\frac{dL_2}{d\varepsilon} \Big|_{\varepsilon=0} = \frac{d}{d\varepsilon} \left(\tilde{\boldsymbol{\lambda}}_x^T \mathbf{g}(\mathbf{x}^*(\tilde{T}) + \varepsilon \delta \mathbf{x}(\tilde{T})) - \tilde{\boldsymbol{\lambda}}_x^T (\mathbf{x}^*(0) + \varepsilon \delta \mathbf{x}(0)) + \tilde{\lambda}_y (y^*(0) + \varepsilon \delta y(0)) \right) \Big|_{\varepsilon=0} \quad (34a)$$

$$\begin{aligned} &= {}_x \boldsymbol{\lambda}^{*T} \frac{\partial \mathbf{g}}{\partial \mathbf{x}_T} \Big|_* \dot{\mathbf{x}}^*(T^*) \delta T + {}_x \boldsymbol{\lambda}^{*T} \frac{\partial \mathbf{g}}{\partial \mathbf{x}_T} \Big|_* \delta \mathbf{x}(T^*) - {}_x \boldsymbol{\lambda}^{*T} \delta \mathbf{x}(0) + {}_y \lambda^* \delta y(0) \\ &+ \delta_x \boldsymbol{\lambda}^T (\mathbf{g}(\mathbf{x}^*(T^*)) - \mathbf{x}^*(0)) + \delta_y \lambda y^*(0), \end{aligned} \quad (34b)$$

$$\frac{dL_3}{d\varepsilon} \Big|_{\varepsilon=0} = \frac{d}{d\varepsilon} \left(\int_0^{T^* + \varepsilon \delta T} \mathcal{H}(\mathbf{w}^* + \varepsilon \delta \mathbf{w}) - (\boldsymbol{\rho}^* + \varepsilon \delta \boldsymbol{\rho})^T (\dot{\mathbf{z}}^* + \varepsilon \delta \dot{\mathbf{z}}) dt \right) \Big|_{\varepsilon=0} \quad (35a)$$

$$= \int_0^{T^* + \varepsilon \delta T} \frac{d}{d\varepsilon} \left(\mathcal{H}(\mathbf{w}^* + \varepsilon \delta \mathbf{w}) - (\boldsymbol{\rho}^* + \varepsilon \delta \boldsymbol{\rho})^T (\dot{\mathbf{z}}^* + \varepsilon \delta \dot{\mathbf{z}}) \right) dt \Big|_{\varepsilon=0} + \left[\mathcal{H}(\mathbf{w}_{T^*}^*) - \boldsymbol{\rho}_{T^*}^{*T} \dot{\mathbf{z}}_{T^*}^* \right] \delta T \quad (35a)$$

$$= \int_0^{T^*} \left(\frac{\partial \mathcal{H}}{\partial \mathbf{w}} \Big|_* \delta \mathbf{w} - \delta \boldsymbol{\rho}^T \dot{\mathbf{z}}^* - \boldsymbol{\rho}^{*T} \delta \dot{\mathbf{z}} \right) dt + \left[\mathcal{H}(\mathbf{w}_{T^*}^*) - \boldsymbol{\rho}_{T^*}^{*T} \dot{\mathbf{z}}_{T^*}^* \right] \delta T \quad (35b)$$

$$\begin{aligned} &= \left[-\boldsymbol{\rho}^{*T} \delta \mathbf{z} \right]_0^{T^*} + \int_0^{T^*} \left(\frac{\partial \mathcal{H}}{\partial \mathbf{w}} \Big|_* \delta \mathbf{w} - \delta \boldsymbol{\rho}^T \dot{\mathbf{z}}^* + \dot{\boldsymbol{\rho}}^{*T} \delta \dot{\mathbf{z}} \right) dt + \left[\mathcal{H}(\mathbf{w}_{T^*}^*) - \boldsymbol{\rho}_{T^*}^{*T} \dot{\mathbf{z}}_{T^*}^* \right] \delta T \\ &= \boldsymbol{\rho}_0^{*T} \delta \mathbf{z}(0) - \boldsymbol{\rho}_{T^*}^{*T} \delta \mathbf{z}(T^*) + \left[\mathcal{H}(\mathbf{w}_{T^*}^*) - \boldsymbol{\rho}_{T^*}^{*T} \dot{\mathbf{z}}_{T^*}^* \right] \delta T \end{aligned} \quad (35c)$$

$$+ \int_0^{T^*} \left(\left[\frac{\partial \mathcal{H}}{\partial \mathbf{z}} \Big|_* + \dot{\boldsymbol{\rho}}^{*T} \right] \delta \mathbf{z} + \frac{\partial \mathcal{H}}{\partial \mathbf{u}} \Big|_* \delta \mathbf{u} + \left[\frac{\partial \mathcal{H}}{\partial \boldsymbol{\rho}} \Big|_* - \dot{\mathbf{z}}^{*T} \right] \delta \boldsymbol{\rho} \right) dt. \quad (35d)$$

where

$$\begin{aligned} \mathbf{Q}^- &= \begin{bmatrix} 0 & (m_h l_o^2 + 2m_l a l_o) \cos(\alpha) \\ 0 & 0 \end{bmatrix} \\ &\quad - m_l a b \begin{bmatrix} 1 & 1 \\ 0 & 1 \end{bmatrix}, \end{aligned} \quad (38b)$$

$$\begin{aligned} \mathbf{Q}^+ &= \begin{bmatrix} m_l b^2 & m_l l_o^2 + m_l a^2 + m_h l_o^2 \\ m_l b^2 & 0 \end{bmatrix} \\ &\quad - m_l b l_o \cos(\alpha) \begin{bmatrix} 1 & 1 \\ 0 & 1 \end{bmatrix}, \end{aligned} \quad (38c)$$

where $\dot{\mathbf{q}}^-$ and $\dot{\mathbf{q}}^+$ are the velocities before and after impact, respectively. Note that the relabeling of coordinates $\mathbf{q}^+ = [\theta_{st} \ \theta_{sw}]^T$ extends the half stride to a complete periodic motion:

$$\mathbf{g}(\mathbf{x}) = \begin{bmatrix} 0 & 1 \\ 1 & 0 \end{bmatrix} \mathbf{q} \\ \left[\mathbf{Q}^+(\mathbf{q})^{-1} \mathbf{Q}^-(\mathbf{q}) \dot{\mathbf{q}} \right]. \quad (39)$$

A.3 Implementation Details for the Direct Method

A.3.1 Transcription of Input Space While we implement the Bézier polynomial in its explicit form:

$$\hat{\mathbf{u}}(t, \xi) = \sum_{j=1}^{n_\xi} \binom{n_\xi - 1}{j - 1} (1 - t)^{n_\xi - j} t^{j-1} \xi_j, \quad (40)$$

the cubic B-spline is defined by the recursion formula due to deBoor, Cox, and Mansfield [Chapter 2.2 in Piegl and Tiller (1997)]:

$$\mathcal{B}_{i,k}(t) := \begin{cases} 1 & \text{if } \tau_i \leq t < \tau_{i+1}, \\ 0 & \text{otherwise,} \end{cases} \quad \text{if } k = 0 \quad (41a)$$

$$\mathcal{B}_{i,k}(t) := \begin{cases} \frac{t - \tau_i}{\tau_{i+k} - \tau_i} \mathcal{B}_{i,k-1}(t) \\ + \frac{\tau_{i+k+1} - t}{\tau_{i+k+1} - \tau_{i+1}} \mathcal{B}_{i+1,k-1}(t) \end{cases}, \quad \text{if } k > 0 \quad (41b)$$

such that

$$\hat{\mathbf{u}}(t, \xi) = \sum_{j=1}^{n_\xi} \mathcal{B}_{j-1, n_{\text{poly}}}(t) \xi_j, \quad (41c)$$

where the polynomial degree $n_{\text{poly}} = 3$ corresponds to the cubic spline. To define the knot points τ_i , we

uniformly separate the time by equidistant time steps $\Delta t = T/n_{\text{seg}}$, where the number of segments is given by $n_{\text{seg}} = n_{\xi} - n_{\text{poly}}$. Requiring the B-spline to be defined in the time interval $[0, T]$, yields the knot points:

$$\tau_i = (i - n_{\text{poly}})\Delta t, \quad \forall i \in \{0, 1, \dots, n_{\tau} - 1\}. \quad (41\text{d})$$

where $n_{\tau} = 2n_{\text{poly}} + n_{\text{seg}}$.

A.3.2 Computation of Sensitivities In addition to the numerical integration of $\hat{x}(T)$ within the equality constraints (32d), the evaluation of the zero-function \hat{r}_{σ} , as defined in equation (32a), depends on sensitivity information based on $\hat{s}^T = [T \ x_0^T \ \xi^T]$. There are three numerical approaches for computing the sensitivities $\partial\hat{c}/\partial\hat{s} \in \mathbb{R}^{1 \times (1+n_x+n_{\xi})}$ and $\partial\hat{h}/\partial\hat{s} \in \mathbb{R}^{(n_x+2) \times (1+n_x+n_{\xi})}$: finite differences, forward sensitivities and adjoint techniques (Sengupta et al. 2014). Generally, finite difference methods require extensive manual tuning of step sizes to achieve the desired accuracy in sensitivity information. In contrast, when using variable step-size solvers, this accuracy is automatically maintained within the solver's tolerances for both forward sensitivities and adjoint techniques. We chose to implement forward sensitivities, which compute the sensitivity of the flow $\partial\hat{z}/\partial\hat{s}$ by simultaneously integrating the dynamics $\dot{z}^T = [\mathbf{f}^T \ l]$ and their derivatives, as described in Dickinson and Gelinas (1976). While forward sensitivities are straightforward to implement, their complexity scales as $\mathcal{O}(n_x n_{\xi})$, which can become computationally expensive when the input parameterization is large ($n_{\xi} \gg n_x$). In such cases, the adjoint method is more efficient, with a complexity of $\mathcal{O}(n_x + n_{\xi})$, as it only provides sensitivity information at the final time T . Since only the sensitivities at the final time T are needed to compute \hat{r}_{σ} , the adjoint method avoids the overhead of forward sensitivity methods, which return sensitivities at all times $t \in [0, T]$.

A.3.3 Second Order Condition To determine whether a zero $\hat{\chi} \in \hat{r}^{-1}(\mathbf{0})$ corresponds to a local minimum or a saddle point, we can examine the matrix $\hat{\mathbf{R}}$, which is obtained as a by-product of applying Newton's Method in Algorithm 1. Introducing the gradient notations $\nabla\hat{c}^T = \frac{\partial\hat{c}}{\partial\hat{s}}$ and $\nabla\hat{h}^T = \frac{\partial\hat{h}}{\partial\hat{s}}$, the Jacobian matrix takes the specific form:

$$\hat{\mathbf{R}} = \begin{bmatrix} \nabla^2\hat{c} + \nabla^2\hat{h}\hat{\lambda} & \hat{h} \\ \hat{h}^T & 0 \end{bmatrix}. \quad (42)$$

Assuming that the equality constraints \hat{h} are regular (i.e., $\nabla\hat{h}$ has full rank), the second-order condition for a local minimum requires the projected Hessian, defined as

$$\begin{aligned} \hat{\mathbf{H}} &= \left(\begin{bmatrix} \mathbf{I} \\ \mathbf{0} \end{bmatrix} \hat{\mathbf{D}} \right)^T \hat{\mathbf{R}} \left(\begin{bmatrix} \mathbf{I} \\ \mathbf{0} \end{bmatrix} \hat{\mathbf{D}} \right) \\ &= \hat{\mathbf{D}}^T \left(\nabla^2\hat{c} + \nabla^2\hat{h}\hat{\lambda} \right) \hat{\mathbf{D}}, \end{aligned} \quad (43)$$

to be positive semi-definite for any $\hat{\mathbf{D}} \in \mathbb{R}^{n_x+n_{\xi}+1 \times n_{\xi}-1}$ that satisfies $\text{span}(\hat{\mathbf{D}}) = \text{null}(\nabla\hat{h}^T)$ (Luenberger and Ye 2021).

In practice, the matrix $\hat{\mathbf{D}}$, containing linearly independent columns, can be constructed using the singular value decomposition (SVD) of $\nabla\hat{h}$. Hence, for a zero $\hat{\chi} \in \hat{r}^{-1}(\mathbf{0})$,

checking the sign of the smallest eigenvalue of $\hat{\mathbf{H}}$ is sufficient to distinguish between a local minimum and a saddle point. This classification can be summarized compactly as:

$$\min(\text{eig}(\hat{\mathbf{H}})) \quad \begin{cases} < 0, & \text{saddle point,} \\ = 0, & \text{local minimum,} \\ > 0, & \text{strict local minimum.} \end{cases} \quad (44)$$